

1 Reviewer 3:

2 This paper used an Extended Response Surface Modeling (ERSM) technique to assess the  
3 source contributions of various chemical precursors, emission sectors, source regions, and  
4 their combinations to the PM<sub>2.5</sub> concentrations over the BTH area. It extended the previous  
5 conventional RSM model and pursued more than 1000 simulation scenarios. It is informative  
6 and valuable to the air pollution controls over the heavily polluted BTH area. I would suggest  
7 this paper to be published after minor revision.

8 Response: We appreciate the reviewer's valuable comments which help us improve the  
9 quality of the manuscript. We have carefully revised the manuscript according to the  
10 reviewers' comments. Point-to-point responses are given below. The original comments are in  
11 black, while our responses are in blue.

12

13 (1) In the abstract, page 2, line 6, "primary inorganic PM<sub>2.5</sub> is the single pollutant which  
14 makes the largest contribution (24-36%) to PM<sub>2.5</sub> concentrations." What is the exact mean of  
15 the word "single"?

16 Response: We thank the reviewer for this valuable comment. In the context of this sentence, a  
17 "single" pollutant means one of the six pollutants (or pollutant groups) considered in the  
18 RSM/ERSM prediction systems, i.e., NO<sub>x</sub>, SO<sub>2</sub>, NH<sub>3</sub>, NMVOC+IVOC, POA, and primary  
19 inorganic PM<sub>2.5</sub>. Primary inorganic PM<sub>2.5</sub> is defined as the chemical components of primary  
20 PM<sub>2.5</sub> other than POA. To avoid confusion, we have revised the preceding sentence as follows  
21 in the revised manuscript (Page 2, Line 5-7).

22 Among all air pollutants, primary inorganic PM<sub>2.5</sub> makes the largest contribution (24-36%)  
23 to PM<sub>2.5</sub> concentrations.

24

25 (2) In the Table S4, "Statistical results for the comparison of monthly PM<sub>2.5</sub> concentrations",  
26 the variable calculated in the statistics is hourly PM<sub>2.5</sub> concentrations, right?

27 Response: The original data used in the statistical analysis are daily PM<sub>2.5</sub> concentrations. We  
28 have clarified this in the footnote of the revised table.

29

30 (3) In Table S4 and S5, please add the number of data pairs, especially in S5.

31 Response: We have added the number of data pairs used in statistics in the revised Table S4  
32 and S5.

33

1 (4) I would suggest the authors add a discussion on the limitations or uncertainties of this  
2 study at the end of the conclusion section.

3 Response: Following the reviewer's suggestion, we have added a paragraph about the  
4 limitations and uncertainties of the present study at the end of the manuscript (Page 21, Line  
5 13-27). The added paragraph is shown as follows.

6 The present study has a few limitations. First, the establishment of ERSM requires several  
7 hundred or over 1000 emission scenarios, although the scenario number needed for a specific  
8 number of control variables has already been dramatically reduced as compared to the  
9 conventional RSM technique. Studies are needed to further reduce the scenario number but  
10 retain the accuracy of the ERSM technique. Second, the current ERSM technique has not  
11 considered the impact of meteorological variations on ambient concentrations. Third,  
12 although the responses of PM<sub>2.5</sub> concentrations to precursor emissions predicted by ERSM  
13 have been demonstrated to agree well with chemical transport model simulations, evaluating  
14 the predicted responses against the actual situation in the real atmosphere still represents a  
15 major challenge, because it is extremely difficult to artificially perturb emissions in the  
16 atmosphere. Last but not the least, the NMVOC and IVOC emissions have been lumped  
17 together in this study to reduce the number of control variables. Considering their differences  
18 in sources and SOA formation potentials, a detailed quantification of the individual  
19 contributions of NMVOC and IVOC emissions from various sources to PM<sub>2.5</sub> concentrations  
20 is required in the future to better inform NMVOC/IVOC control policies.

1 Reviewer 2:

2 We thank the referee for a thoughtful and detailed review of our manuscript. Incorporation of  
3 the reviewer's suggestions has led to a much improved manuscript. Below we provide a  
4 point-by-point response to the reviewer's comments and summarize the changes that have  
5 been incorporated in the revised manuscript.

6

7 General comments

8 ERSM has been developed by extending the capabilities of the conventional RSM. Its  
9 performance was evaluated. Then, sensitivities of emissions of various primary pollutants and  
10 precursors, sectors, and regions on seasonal concentrations of PM<sub>2.5</sub> and their components in  
11 BTH region were discussed.

12 The advantage of the ERSM technique is that it can represent complex non-linear  
13 relationships between ambient pollutant concentrations and their precursor emissions. On the  
14 other hand, it requires over 1000 simulations. If changes in ambient concentrations in several  
15 future scenarios, only several simulations with the brute force method are required. I feel the  
16 advantage of the ERSM which overcome tremendous efforts to run simulations over 1000  
17 times is not fully emphasized in this manuscript. In addition, descriptions of limitations of the  
18 ERSM technique are scarce. Please add more descriptions on the advantage and disadvantage  
19 of the ERSM technique.

20 Response: We appreciate the reviewer's valuable comment. The ERSM technique has several  
21 advantages over the traditional brute force method. First, the ERSM technique is able to  
22 characterize the nonlinearity in the relationships between ambient concentrations and air  
23 pollutant emissions. Second, cost-effective emission controls need to optimize over various  
24 pollutants from multiple regions and sectors. Using the brute force method, we need to  
25 repeatedly adjust the control option combinations and run the chemical transport model for  
26 numerous times. In contrast, the ERSM prediction system, once built, enables real-time  
27 prediction of PM<sub>2.5</sub> concentrations for any given control strategy and proves to be an efficient  
28 and user-friendly decision making tool. Third, ERSM can be applied to design least-cost  
29 control strategy once it is coupled with control cost models/functions that links the emission  
30 reductions with economic costs.

31 The major disadvantage of the ERSM technique is that it requires several hundred or over  
32 1000 emission scenarios, although the scenario number needed to build the response surface  
33 for a specific variable number has already been dramatically reduced as compared to the  
34 conventional RSM technique. Future studies are needed to further reduce the scenario number  
35 and still retain the accuracy of the ERSM technique. Another disadvantage is that the current  
36 ERSM technique does not consider the impact of meteorological variations on ambient  
37 concentrations. We have detailed the advantages and disadvantages of the ERSM technique in  
38 the revised manuscript (Page 4, Line 12-15; Page 8, Line 5-10; Page 21, Line 13-18).

1

2 ERSM could provide valuable information to develop effective strategies based on complex  
3 non-linear relationships. It means non-linear responses should represent the actual situation in  
4 the real atmosphere. I think validation of the responses obtained by ERSM is not enough  
5 whereas comparisons of observed concentrations have been made.

6 Especially, nonlinear responses of NO<sub>x</sub> emissions are critical for policy making. How much  
7 NO<sub>x</sub> reduction is necessary to realize positive effects to reduce PM<sub>2.5</sub> concentrations?  
8 ERSM could give the answer. However, if the answer is not correct in the real atmosphere,  
9 policies may fail to realize PM<sub>2.5</sub> reductions.

10 Response: We thank the reviewer for this valuable comment. We fully agree that the  
11 validation of the responses predicted by ERSM is very important. In response to the comment,  
12 we (1) strengthen the validation of the ERSM-predicted responses against CMAQ/2D-VBS  
13 simulation, (2) add some discussions about the evaluation of CMAQ/2D-VBS-simulated  
14 responses against the actual situation in the real atmosphere, and (3) add some discussions  
15 about the impact of NO<sub>x</sub> emission reductions.

16 (1) In the revised manuscript, we have added a group of scatter plots comparing the PM<sub>2.5</sub>  
17 responses (i.e., difference between PM<sub>2.5</sub> concentration in an emission control scenario and  
18 that in the base case) predicted by ERSM and independent CMAQ/2D-VBS simulations  
19 (second row of Fig. 2, shown below). Moreover, we have calculated the statistics for the  
20 comparison of PM<sub>2.5</sub> responses (Table 2, also shown below). Figure 2 and Table 2 illustrate  
21 that the ERSM-predicted and CMAQ/2D-VBS-simulated PM<sub>2.5</sub> responses agree well with  
22 each other. The correlation coefficients are larger than 0.99, and the normalized mean errors  
23 (NMEs) are within 5.6% for all four months. Note that we did not show the normalized errors  
24 (NEs) and mean normalized errors (MNEs) for PM<sub>2.5</sub> responses as we did for PM<sub>2.5</sub>  
25 concentrations in Table 2. The reason is that the CMAQ/2D-VBS-simulated PM<sub>2.5</sub> responses  
26 are very close to zero in several scenarios which are randomly generated, therefore their  
27 normalized errors (NEs) and mean normalized errors (MNEs) could be extremely large even  
28 if the absolute errors are small, which cannot properly characterize the accuracy of the ERSM  
29 technique.

30 In addition, we compare the 2D-isopleths of PM<sub>2.5</sub> concentrations as a function of  
31 continuous changes in precursor emissions (including NO<sub>x</sub> emissions) in a full range (from 0  
32 to 1.2 times), derived from the ERSM and conventional RSM techniques (Fig. 3 in the  
33 manuscript). The predictions by conventional RSM can be regarded as proxies for real  
34 CMAQ/2D-VBS simulations since it has been extensively demonstrated to have high  
35 accuracy and stability in previous studies (Xing et al., 2011; Wang et al., 2011b). For this  
36 reason, the comparison between the ERSM and conventional RSM techniques helps to  
37 evaluate the accuracy and stability of the ERSM technique. The comparison shows that the  
38 shapes of isopleths derived from both prediction systems agree well with each other except  
39 for a few cases with very large emission reductions (> 80%), demonstrating the reliability of

1 ERSM in predicting the responses of PM<sub>2.5</sub> concentrations to changes in emissions of  
2 precursors, including NO<sub>x</sub>. Note that all sensitivity scenarios used in the “Results and  
3 discussion” section have emission reductions ≤ 80%, therefore, the results and conclusions of  
4 this study are not affected by the relatively large errors at very large emission reductions.

5 (2) The preceding discussions demonstrate the agreement between ERSM-predicted and  
6 CMAQ/2D-VBS-simulated PM<sub>2.5</sub> responses. However, evaluating the PM<sub>2.5</sub> responses  
7 simulated by chemical transport models against the actual situation in the real atmosphere  
8 represents a major challenge in atmospheric modeling studies, because it is extremely difficult  
9 to artificially perturb emissions in the real atmosphere. Some special events when temporary  
10 control measures are implemented, such as the Beijing Olympic Games and the APEC  
11 conference, might provide opportunities to evaluate the simulated responses. However, such  
12 effects of temporary emission reductions could be confounded by meteorological variations.  
13 We fully recognize the importance to make sure that the simulated responses represent the  
14 situation in real atmosphere, but such evaluations are very complicated and appear to be  
15 beyond the purview of the present study. We have highlighted this issue as a major limitation  
16 of the present study (Page 21, Line 8-12), which requires further investigations.

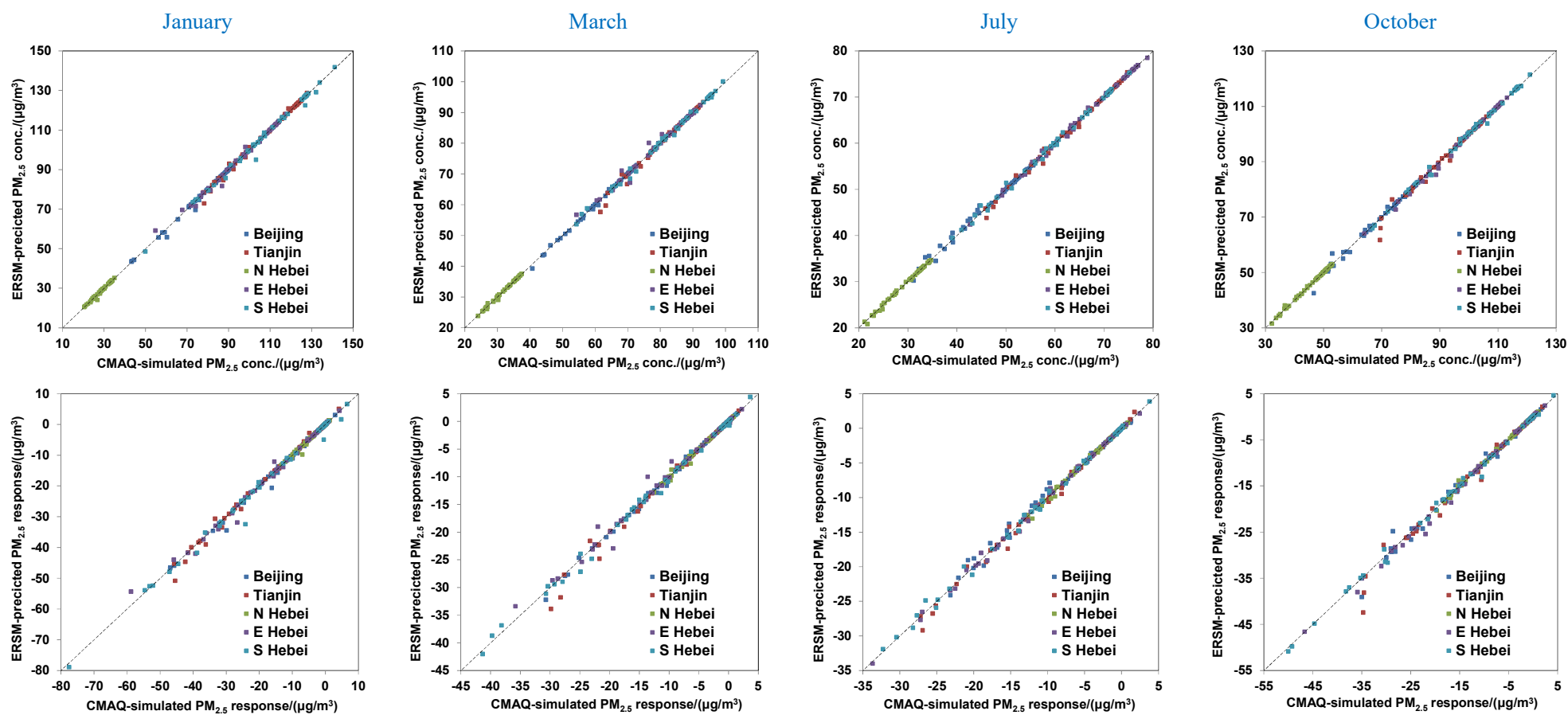


Figure 2. Comparison of  $PM_{2.5}$  concentrations (top row) and  $PM_{2.5}$  responses (bottom row) predicted by the ERSM technique with out-of-sample CMAQ/2D-VBS simulations. The dashed line is the one-to-one line indicating perfect agreement.

Table 2. Comparison between ERSM-predicted and CMAQ/2D-VBS-simulated PM<sub>2.5</sub> concentrations for 54 out-of-sample scenarios.

Month	Variable	Statistical index	Beijing	Tianjin	Northern Hebei	Eastern Hebei	Southern Hebei	
Jan	PM <sub>2.5</sub> concentration	R	0.998	0.998	0.995	0.997	0.997	
		MNE (%)	0.52	0.55	0.64	0.67	0.60	
		Maximum NE (%)	7.56	6.98	10.67	8.01	8.03	
		95% percentile of NEs (%)	1.61	2.86	2.92	3.46	3.02	
		NME (%)	0.44	0.46	0.57	0.53	0.53	
	PM <sub>2.5</sub> response	R	0.998	0.998	0.995	0.997	0.997	
		NME (%)	3.36	3.48	4.25	4.00	3.88	
	Mar	PM <sub>2.5</sub> concentration	R	0.999	0.996	0.998	0.995	0.999
			MNE (%)	0.37	0.54	0.39	0.57	0.49
			Maximum NE (%)	3.75	6.58	4.30	5.04	3.22
95% percentile of NEs (%)			1.53	3.15	2.03	4.35	2.03	
NME (%)			0.31	0.45	0.34	0.49	0.42	
PM <sub>2.5</sub> response		R	0.999	0.996	0.998	0.995	0.999	
		NME (%)	2.38	4.32	2.70	4.55	3.59	
Jul		PM <sub>2.5</sub> concentration	R	0.997	0.998	0.998	0.999	0.999
			MNE (%)	0.94	0.54	0.46	0.37	0.47
			Maximum NE (%)	5.05	5.02	4.65	1.83	3.62
	95% percentile of NEs (%)		3.47	2.33	2.17	1.49	1.87	
	NME (%)		0.80	0.47	0.41	0.33	0.39	
	PM <sub>2.5</sub> response	R	0.997	0.998	0.998	0.999	0.999	
		NME (%)	4.97	3.71	2.80	2.58	2.78	
	Oct	PM <sub>2.5</sub> concentration	R	0.996	0.994	0.999	0.999	0.999
			MNE (%)	0.83	0.70	0.36	0.39	0.36
			Maximum NE (%)	8.90	11.19	3.79	3.90	2.46
95% percentile of NEs (%)			3.04	3.50	1.44	2.10	1.64	
NME (%)			0.67	0.58	0.30	0.35	0.32	
PM <sub>2.5</sub> response		R	0.996	0.994	0.999	0.999	0.999	
		NME (%)	4.51	5.64	2.20	3.29	2.79	

(3) Next we discuss the impact of NO<sub>x</sub> emission reductions. If only the NO<sub>x</sub> emissions within the BTH region are controlled, our simulation results (Fig. 4) reveal that a very large reduction ratio (about 80%) is required to realize a reduction in annual PM<sub>2.5</sub> concentrations in most areas. However, the effects could be distinctly different if NO<sub>x</sub> emissions outside the BTH region are jointly reduced. Our previous studies using the CMAQ model (Zhao et al., 2013b; Wang et al., 2010; Wang et al., 2011b) have shown that uniform reductions in NO<sub>x</sub> emissions in the whole China by 23-50% result in considerable annual PM<sub>2.5</sub> reduction over the BTH region. This is because NO<sub>x</sub> emission reductions in upwind regions are more likely to result in a net

PM<sub>2.5</sub> decrease compared with local emission reductions, since the photochemistry typically changes from a NMVOC-limited regime in local urban areas at surface to a NO<sub>x</sub>-limited regime in downwind areas or at upper levels (Xing et al., 2011). The simulation results in this paper also support the above-mentioned pattern and mechanism to some extent: even a 20% NO<sub>x</sub> emission reduction in BTH can lead to PM<sub>2.5</sub> decrease in Northern Hebei (see Fig. 4 in the manuscript), because, as the northernmost region in BTH, it is significantly affected by emissions in other regions within BTH. In view of the discussions above, we suggest that NO<sub>x</sub> emissions should be substantially reduced in the long run in both the BTH region and the other parts of China.

Finally, we note that NO<sub>x</sub> emissions were recently found to oxidize SO<sub>2</sub> in aerosol water, leading to additional PM<sub>2.5</sub> formation (Cheng et al., 2016; Wang et al., 2016), which is a missing chemical process in most chemical transport models. Incorporation of this process in the model may affect the simulated response of PM<sub>2.5</sub> to NO<sub>x</sub> emissions. More studies are still needed to further investigate the effects of NO<sub>x</sub> emissions on PM<sub>2.5</sub> concentrations. We have added the discussions above in the revised manuscript (from Page 10, Line 29 to Page 11, Line 3; Page 11, Line 10-32; Page 21, Line 18-23; from Page 13, Line 21 to Page 14, Line 6).

Which components are included in inorganic PM<sub>2.5</sub>? Is EC included? How about other components like metals? It looks strange that primary organic aerosol (POA) is included as a precursor probably due to treatment in VBS. Please give precise definitions of these words.

Response: We thank the reviewer for this valuable comment. Primary inorganic PM<sub>2.5</sub> is defined as all chemical components of primary PM<sub>2.5</sub> other than POA. By definition, it includes EC, metals, as well as many other constituents such as sulfate and nitrate directly emitted from sources. POA is treated as a precursor because it undergoes chemical reactions and produces SOA in the CMAQ/2D-VBS model, while primary inorganic PM<sub>2.5</sub> is chemically inert. In the revised manuscript, we have defined the “primary inorganic PM<sub>2.5</sub>” clearly and added the reasons to treat POA as a precursor (from Page 8, Line 28 to Page 9, Line 1).

What do “discrepant temporary control strategies” mean? How are they possible? I understand major sources are different in each heavy air pollution episode. However, it could be possible to implement different temporary control strategies for each episode only if it could be forecasted. Can ERSM be used to forecast major sources in coming heavy air pollution episodes? I think differences of major sources in each episode suggest to implement strategies which control emissions of all the sources which could be major in various episodes.

Response: “Discrepant temporary control strategies” mean that the temporary control strategies should focus on different emission sources during different heavy pollution episodes. To make it clear, we have revised this sentence as follows:



The source contribution features for various types of heavy-pollution episodes are distinctly different from each other, and from the monthly mean results, illustrating that control strategies should be differentiated based on the major contributing sources during different types of episodes. (Page 2, Line 21-24)

In the present study, we only studied the source contribution features of three typical episodes. These results are not yet sufficient to guide the development of temporary control strategies for all heavy-pollution episodes, because the conclusions drawn from the three episodes may not be generalized to pollution types. In future studies, we need to simulate more episodes to improve their classification and to comprehensively understand the source contribution features of each pollution type. For a coming heavy-pollution episode, we can predict its pollution type using an air quality forecasting model, and subsequently formulate the temporary control strategies based on the source contribution features of this specific pollution type. We have described the method to develop episode-specific control strategies using ERSM in the revised manuscript (Page 19, Line 14-23).

#### Specific comments

Page 3, Line 8 How much are 2012 levels?

Response: It was not until January 2013 that the Ministry of Environment of China began to report PM<sub>2.5</sub> concentrations to the public. In 2012, the PM<sub>2.5</sub> concentrations were only available for limited sites such as the United States Embassy in Beijing, where the annual mean concentration was 90.7 µg/m<sup>3</sup>. The average PM<sub>2.5</sub> concentrations over the BTH region were not publicly available.

Page 3, Line 22 The sentence here says “CTMs are the only feasible tools for evaluating the response of PM<sub>2.5</sub> concentrations to emission changes”. However, the sentences around the line 14 describe that embedding chemical tracers in chemical transport models (CTMs) cannot represent non-linear response. They may confuse some readers who are not familiar to CTMs.

Response: We agree with the reviewer and have deleted the former sentence, which is redundant.

Page 3, Line 26 “Sensitivities” are more appropriate than “contributions” in the context here.

Response: We agree with the reviewer and have modified this sentence as follows in the revised manuscript (Page 3, Line 25-31).

A number of studies have utilized the “Brute force” method to quantify the sensitivities of PM<sub>2.5</sub> concentrations over the BTH region to emissions from different spatial regions or different economic sectors, either on a seasonal basis or during a specific heavy-pollution episode.

Page 4, Line 5 How inadequate?

Response: The previous studies reviewed here applied the Decoupled Direct Method or Adjoint Analysis approach, which are used to calculate first-order sensitivities. However, characterizing the nonlinearity in the responses of PM<sub>2.5</sub> concentrations to emissions requires the calculation of second- or higher-order sensitivities. Therefore, we state that the previous studies have inadequately captured the nonlinearity in the responses of PM<sub>2.5</sub> concentrations to emissions. We have added the explanations to the revised manuscript (Page 4, Line 5-8).

Page 5, Line 7 How were emissions of IVOC provided?

Response: Following our previous study (Zhao et al., 2016), we assume IVOC emissions to be 30 times, 4.5 times, 1.5 times, and 3.0 times the POA emissions from gasoline vehicles, diesel vehicles, biomass burning, and other emission sources, respectively, which is based on a series of laboratory measurements (Gordon et al., 2014b; Gordon et al., 2014a; Hennigan et al., 2011; Jathar et al., 2014). We have added these descriptions in the revised manuscript (from Page 6, Line 32 to Page 7, Line 4).

Page 5, Line 8 OA and SOA are listed parallelly, but SOA is included in OA.

Response: We have revised the sentence as follows (Page 5, Line 6-11).

Compared with the default CMAQ, the CMAQ/2D-VBS model explicitly simulates aging of secondary organic aerosol (SOA) formed from non-methane volatile organic compounds (NMVOC), aging of primary organic aerosol (POA), and photo-oxidation of intermediate-volatility organic compounds (IVOC), thereby significantly improving the simulation results of organic aerosol (OA), particularly SOA.

Page 5, Line 30 I think NCEP final analysis data is not reanalysis data. Is it not used for grid nudging?

Response: We have revised the descriptions about the first guess field and nudging as follows in order to make them more accurate.

The National Center for Environmental Prediction (NCEP)'s FNL (Final) Operational Global Analysis data (ds083.2) at  $1.0^\circ \times 1.0^\circ$  and 6-h resolution are used to generate the first guess field. The NCEP's Automated Data Processing (ADP) data (ds351.0 and ds461.0) are used in objective analysis (i.e., grid nudging). (from Page 5, Line 31 to Page 6, Line 2 in the revised manuscript)

Page 6, Line 4 I think terrain data is not from MODIS.

Response: We apologize for the mistake and have corrected this sentence as follows:

The land cover type data are obtained from the Moderate resolution Imaging Spectroradiometer (MODIS). (Page 6, Line 7-8 in the revised manuscript)

Page 6, Line 25 How about open biomass burning emissions?

Response: In both the BTH and national emission inventories, the emissions from open burning of agricultural residue are calculated using crop yields, straw to grain ratio, fraction of biomass burned in the open field, and emission factors (Fu et al., 2013; Zhao et al., 2013a; Wang and Zhang, 2008). We do not include the emissions from forest and grassland fires, which typically account for less than 5% of the total biomass burning emissions over the BTH region (Qin and Xie, 2011) and are not the focus of the present study. We have added the preceding descriptions in the revised manuscript (Page 6, Line 23-28).

Page 9, Line 21 How about the performance of  $\text{SO}_4^{2-}$ ,  $\text{NO}_3^-$ , and OA?

Response: This manuscript focuses on the response of  $\text{PM}_{2.5}$  concentrations to air pollutant emissions, and the responses of  $\text{SO}_4^{2-}$ ,  $\text{NO}_3^-$ , and OA are examined just to better understand the responses of  $\text{PM}_{2.5}$ . For this reason, the response surfaces of  $\text{SO}_4^{2-}$ ,  $\text{NO}_3^-$ , and OA are only built using the conventional RSM technique to map their concentrations versus emissions of five  $\text{PM}_{2.5}$  precursors, i.e.,  $\text{NO}_x$ ,  $\text{SO}_2$ ,  $\text{NH}_3$ ,  $\text{NMVOC}+\text{IVOC}$ , and POA. Since conventional RSM has been adequately demonstrated to have high accuracy and stability (Xing et al., 2011; Wang et al., 2011b), we did not include its validation in the present paper. We have clarified this point in the revised manuscript (Page 8, Line 18-22; Page 9, Line 27-29).

Page 10, Line 8 Why are only NMEs shown? How about R and MNEs? I suppose it is more important for RSM to see responses than to reproduce concentrations.

Response: We fully agree with the reviewer that the evaluation of  $PM_{2.5}$  responses is very important. Since the CMAQ/2D-VBS-simulated  $PM_{2.5}$  responses are very close to zero in several out-of-sample scenarios which are generated randomly, their normalized errors (NEs) and mean normalized errors (MNEs) could be extremely large even if the absolute errors are small, which cannot properly characterize the accuracy of the ERSM technique. For example, for the 11<sup>th</sup> case used in out-of-sample validation, the CMAQ/2D-VBS-simulated  $PM_{2.5}$  response in January is  $0.0003 \mu\text{g}/\text{m}^3$  while the ERSM-predicted value is  $0.03 \mu\text{g}/\text{m}^3$ . While the ERSM-predicted and CMAQ/2D-VBS-simulated values are actually quite close, the NE is as large as about 10000%. Therefore, we argue that NE and MNE are not suitable for evaluating ERSM's performance on  $PM_{2.5}$  responses. With respect to R, the values for  $PM_{2.5}$  responses are exactly the same as those for  $PM_{2.5}$  concentrations, so we did not include R for  $PM_{2.5}$  responses in the original manuscript. In the revised manuscript, we have added R for  $PM_{2.5}$  responses to make the results more clear (Table 2), and also explained the reasons for excluding NE and MNE (from Page 10, Line 30 to Page 11, Line 1).

Page 10, Line 15 I do not understand meaning of comparisons between ERSM and conventional RSM. Why these two model could produce different results? Which should be correct? The sentence in the line 31 says that the ERSM predictions are definitely subject to numerical errors, but I do not know why "definitely". Although there are descriptions of ERSM in the first paragraph of the section 2.2, the advantages and disadvantages of ERSM against conventional RSM should be clearly explained.

Response: We thank the reviewer for this valuable comment. While the conventional RSM has been demonstrated to have very high accuracy and stability, the number of emission scenarios required to build it depends on the variable number via an equation of fourth or higher order. Therefore, the required scenario number would be tens of thousands for over 15 variables and even hundreds of thousands for over 25 variables, which is computationally impossible for most three-dimensional CTMs and proves to be a major limitation for the conventional RSM technique. The ERSM technique substantially reduces the number of scenarios needed to build the response surface by introducing several additional assumptions with respect to the inter-regional transport of air pollutants (see Section 2.2), which extends its applicability to a much larger number of regions, pollutants, and sectors with an acceptable computational burden. Meanwhile, the additional assumptions in the ERSM techniques might affect its accuracy. Therefore, the conventional RSM technique is theoretically more close to the predictions of CMAQ/2D-VBS, and its accuracy has been extensively evaluated in previous studies (Xing et al., 2011; Wang et al., 2011b). For this reason, the comparison between the ERSM and conventional RSM techniques helps to evaluate the accuracy and stability of the ERSM technique.

The statement that “ERSM predictions are definitely subject to numerical errors” means that ERSM, like all models, cannot exactly agree with the true values. We have deleted this redundant sentence in the revised manuscript to avoid misunderstanding.

As described above, the major advantage of ERSM over conventional RSM is that it is applicable to a much larger number of regions, pollutants, and sectors with an acceptable computational burden. For example, in the present study, the conventional RSM is applied to only 5 control variables, i.e., the total emissions of five PM<sub>2.5</sub> precursors. The ERSM technique, however, is applied to 55 control variables including the emissions of multiple pollutants from different regions and sectors. The major disadvantage of ERSM is that it might be subject to larger errors than conventional RSM due to the additional assumptions in the treatment of inter-regional transport.

We have added the descriptions above in the revised manuscript (Page 4, Line 19-27; Page 11, Line 10-17).

Page 11, Line 5 What is the advantage of ERSM against conventional RSM in the results shown in Figure 4? I think the sector-wise results shown in the right figure cannot be obtained by conventional RSM. Is that correct? Please described what is newly obtained by using ERSM.

Response: It is correct. The sector-wise results shown in Fig. 4 (right panel) and Fig. 5, as well as the regional contributions shown in Fig. 6 can only be obtained from ERSM. We have clarified this in the revised manuscript (Page 12, Line 15-17).

Page 11, Line 16 It looks strange to represent primary inorganic PM<sub>2.5</sub> as “single pollutant” because it is a mixture of various components in fact.

Response: We have modified this sentence as follows:

While primary inorganic PM<sub>2.5</sub> makes the largest contribution to PM<sub>2.5</sub> concentrations among all air pollutants, the total contributions of all precursors (NO<sub>x</sub>, SO<sub>2</sub>, NH<sub>3</sub>, NMVOC, IVOC, and POA), which range between 31% and 48%, exceed that of primary inorganic PM<sub>2.5</sub> (24-36%). (Page 12, Line 25-28)

Page 11, Line 29 What is the reasons of small sensitivities of SO<sub>2</sub> emissions on PM<sub>2.5</sub>?

Response: In the manuscript, we state that the PM<sub>2.5</sub> sensitivity to SO<sub>2</sub> emissions is smaller than that to POA, NMVOC+IVOC, and NH<sub>3</sub>. From 2007 to 2014 (the base year of this study), both SO<sub>2</sub> emissions and SO<sub>4</sub><sup>2-</sup> concentrations in PM<sub>2.5</sub> have been continuously decreasing due to

effective control policies (Wang et al., 2017). As a result, the simulated concentrations of  $\text{SO}_4^{2-}$  are much lower than those of OA (see Fig. 7 and Fig. S7 in the manuscript), which explains the smaller sensitivity of  $\text{PM}_{2.5}$  to  $\text{SO}_2$  than those to POA and NMVOC+IVOC. The reason why  $\text{PM}_{2.5}$  is less sensitive to  $\text{SO}_2$  emission reductions than that to  $\text{NH}_3$  is that the reduction in  $\text{NH}_3$  emissions affects both the concentrations of  $\text{NO}_3^-$  and  $\text{SO}_4^{2-}$ , while  $\text{SO}_2$  emission reductions mainly lead to decrease in  $\text{SO}_4^{2-}$  concentrations. Additionally, the small sensitivities to  $\text{SO}_2$  emissions may also be partly attributed to the underestimation of  $\text{SO}_4^{2-}$  in the CMAQ/2D-VBS model, which is a common problem of many chemical transport models (Wang et al., 2011a; Gao et al., 2014; Wang et al., 2013). While the reasons for underestimation are yet to be resolved, possible causes could be the lack of some chemical formation pathways in the modeling system, such as  $\text{SO}_2$  heterogeneous reactions on the dust surface and the oxidation of  $\text{SO}_2$  by  $\text{NO}_2$  in aerosol water (Wang et al., 2013; Fu et al., 2016; Cheng et al., 2016). We have added the discussions in the revised manuscript (Page 13, Line 8-11; Page 14, Line 2-6).

Page 11, Line 31 Nonlinear sensitivities of NO<sub>x</sub> emissions and their changes from negative to positive are described from here. I also agree that this is very important phenomena to consider effective emission controls. However, on the other hand, the descriptions in the page 10 treat such a nonlinear change in sensitivities and differences with conventional RSM as just a rare case involving large unrealistic reduction of NO<sub>x</sub> emissions. I do not agree that. Even if large NO<sub>x</sub> reduction is required, the performance of ERSM to represent such a nonlinear change should be carefully evaluated.

Response: We agree with the reviewer that we should carefully evaluate the performance of ERSM over a full emission range, including at very large NO<sub>x</sub> emission reductions. The reason why we stated that the relatively large errors at very low emission ratios did not affect our conclusion is that all sensitivity scenarios used in the “Results and discussion” section have emission ratios  $\geq 0.2$ . In response to the reviewer’s comment, we have strengthened the validation of ERSM-predicted  $\text{PM}_{2.5}$  responses against CMAQ/2D-VBS simulations, as described in detail in our response to the reviewer’s second “general comment”. On the other hand, we have added a detailed discussion about the relatively large errors at very low NO<sub>x</sub>/NH<sub>3</sub> emission ratios ( $< 0.2$ ), and highlighted the need for further studies (from Page 11, Line 24 to Page 12, Line 6). The revised text is shown below.

The agreement is very good for the case of VOC+IVOC vs POA, and for the cases of NO<sub>x</sub> vs NH<sub>3</sub> and SO<sub>2</sub> vs NH<sub>3</sub> when the emission ratios for NO<sub>x</sub> and NH<sub>3</sub> are larger than 0.2. Relatively large errors occur at very low NO<sub>x</sub>/NH<sub>3</sub> emission ratios ( $< 0.2$ ) due primarily to an extremely strong nonlinearity. Within these low emission ranges, the ERSM technique can capture the general trends in  $\text{PM}_{2.5}$  concentrations in response to emission changes, but the concentration gradients predicted by ERSM are smaller than those given by conventional RSM. More studies are needed to further improve the performance of ERSM at very low NO<sub>x</sub>/NH<sub>3</sub> emission ratios.

Finally, we note that all sensitivity scenarios used in the “Results and discussion” section have emission ratios  $\geq 0.2$ , therefore, the results and conclusions of this study are not affected by the relatively large errors at very low  $\text{NO}_x/\text{NH}_3$  emission ratios.

Page 12, Line 2 Indeed, the regimes are very important for negative and positive sensitivities of  $\text{NO}_x$  emissions. Therefore, it is quite important to see if ERSM could accurately represent regimes in the real atmosphere. I suppose such validations are scarce.

Response: Although the ERSM-predicted responses of  $\text{PM}_{2.5}$  concentrations have been demonstrated to agree fairly well with CMAQ/2D-VBS simulations, evaluating the simulated  $\text{PM}_{2.5}$  responses (or chemical regimes) against the actual situation in the real atmosphere represents a major challenge in atmospheric modeling studies, because it is extremely difficult to artificially perturb emissions in the real atmosphere. Some special events when temporary control measures are implemented, such as the Beijing Olympic Games and the APEC conference, might provide opportunities to evaluate the simulated responses. However, such effects of temporary emission reductions could be confounded by meteorological variations. We fully recognize the importance to make sure that the simulated responses represent the situation in real atmosphere, but such evaluations are very complicated and appear to be beyond the purview of the present study. We have highlighted this issue as a major limitation of the present study (Page 21, Line 18-23), which requires further investigations.

Page 12, Line 20 Are there any discussions on differences between sensitivities of all pollutants and sectors and sum of sensitivities of individual pollutants and sectors?

Response: The sum of sensitivities of  $\text{PM}_{2.5}$  concentrations to individual pollutant-sector combinations is mostly larger than the sensitivity to all pollutants and sectors, especially under large reduction ratios. This is mainly attributed to the overlapping effect of two precursors (e.g.,  $\text{SO}_2$  and  $\text{NH}_3$ ) involved in the formation of ammonium sulfate and ammonium nitrate. Nevertheless, at small reduction ratios, the sum of individual sensitivities is sometimes smaller, because the negative effects of reducing  $\text{NO}_x$  are mitigated when we simultaneously reduce  $\text{NO}_x$  emissions from multiple sectors as well as emissions of other air pollutants such as NMVOC. We have included these discussions in the revised manuscript (Page 14, Line 11-18).

Page 12, Line 31 What is a reason of higher sensitivities of residential and commercial sources in winter? Heating?

Response: There are two major reasons. On one hand, as the reviewer points out, the emissions from residential and commercial sources are relatively higher in winter due to heating. On the



other hand, the weaker vertical mixing in winter also results in a larger relative contribution of low-level sources including the residential and commercial sector. We have added these explanations in the revised manuscript (Page 14, Line 29-32).

Page 13, Line 8 Are there any specific results indicating the importance of NO<sub>x</sub> emissions outside the BTH region?

Response: The present study focuses on the response of PM<sub>2.5</sub> concentrations to emissions within the BTH region. If only the NO<sub>x</sub> emissions within the BTH region are controlled, a very large reduction ratio of about 80% is required to realize a reduction in annual PM<sub>2.5</sub> concentrations in most areas (Fig. 4). However, our previous studies using the CMAQ model (Zhao et al., 2013b; Wang et al., 2010; Wang et al., 2011b) have shown that uniform reductions in NO<sub>x</sub> emissions in the whole China by 23-50% result in considerable annual PM<sub>2.5</sub> reduction over the BTH region, implying the important role of NO<sub>x</sub> emission reductions outside the BTH region. The reason why NO<sub>x</sub> emission reductions in upwind regions are more likely to result in a net PM<sub>2.5</sub> decrease compared with local emission reductions is that the photochemistry typically changes from a NMVOC-limited regime in local urban areas at surface to a NO<sub>x</sub>-limited regime in downwind areas or at upper levels (Xing et al., 2011). The simulation results in this paper also support the above-mentioned pattern and mechanism to some extent: even a 20% NO<sub>x</sub> emission reduction in BTH can lead to PM<sub>2.5</sub> decrease in Northern Hebei (see Fig. 4 in the manuscript), because, as the northernmost region in BTH, it is significantly affected by emissions in other regions within BTH. We have added these discussions in the revised manuscript (from Page 13, Line 21 to Page 14, Line 2).

Page 14, Line 6 How does seasonal variations of NH<sub>3</sub> emissions look like?

Response: The monthly variations in NH<sub>3</sub> emissions from fertilizer application are based on our previous simulation results (Fu et al., 2015) using an agricultural fertilizer modeling system which couples a regional air quality model (the Community Multi-scale Air Quality model, or CMAQ) and an agro-ecosystem model (the Environmental Policy Integrated Climate model, or EPIC). The monthly variations of livestock farming are obtained from Huang et al. (2012), and those of other emission sources are consistent with the descriptions in our previous paper (Wang et al., 2011a). Overall, the monthly variations in total NH<sub>3</sub> emissions are illustrated in the following figure.



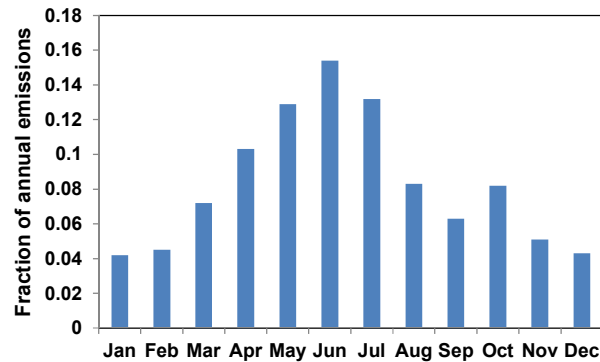


Figure. Monthly variations in total NH<sub>3</sub> emissions over the BTH region.

Page 14, Line 25 Is it confirmed that NO<sub>x</sub> competes with SO<sub>2</sub> for NH<sub>3</sub> in a thermodynamic pathway? I think SO<sub>4</sub><sup>2-</sup> is much more predominantly in aerosol phase than NO<sub>3</sub><sup>-</sup>.

Response: We agree that NH<sub>3</sub> tends to react with SO<sub>2</sub> to form ammonium sulfate. In the present study, the response of SO<sub>4</sub><sup>2-</sup> concentrations to NO<sub>x</sub> emissions can be well explained by only the changes in O<sub>3</sub> and HO<sub>x</sub> concentrations, i.e., the photochemical pathway. Also, the BTH region has been shown to be generally under an NH<sub>3</sub>-rich condition (Wang et al., 2011b). Therefore, the competition between NO<sub>x</sub> and SO<sub>2</sub> for NH<sub>3</sub> does not appear to play a noticeable role in changing SO<sub>4</sub><sup>2-</sup> concentrations. In the revised manuscript, we have deleted the descriptions about the thermodynamic pathway and focused on the photochemical pathway.

Page 15, Line 1 Does this POA include semivolatile components which could condensate only under lower temperature in winter?

Response: We agree with the reviewer that POA includes some semi-volatile components which tend to partition to the particle phase under low temperature in January, which partly explains the higher contributions of POA emissions to OA concentrations in January. Besides, some other factors account for the higher contributions of POA emissions in January and higher contributions of NMVOC+IVOC emissions in July. First, the POA emissions are relatively higher in January due to residential heating, while the NMVOC emissions from solvent use and biogenic sources are higher in July. Second, higher temperature and stronger radiation in July accelerate the formation of SOA from NMVOC+IVOC. We have added the explanations in the revised manuscript (Page 17, Line 3-9).

Page 17, Line 10 I agree more model simulations of more episodes are necessary, but a model can always give results. I believe what is important is to confirm model results are consistent

with actual situations in the real atmosphere. That is quite important to consider effective strategies for heavy air pollutions.

Response: We appreciate the reviewer's valuable comment. We have discussed the validation of PM<sub>2.5</sub> responses predicted by ERSM in detail in our response to the reviewer's second "general comment". In brief, we strengthened the validation of ERSM-predicted responses against CMAQ/2D-VBS simulations and have demonstrated that the ERSM-predicted and CMAQ/2D-VBS-simulated responses of PM<sub>2.5</sub> concentrations to precursor emissions, including NO<sub>x</sub> emissions, agree fairly well with each other. However, evaluating the PM<sub>2.5</sub> responses simulated by CMAQ/2D-VBS against the actual situation in the real atmosphere represents a major challenge in atmospheric modeling studies, because it is extremely difficult to artificially perturb emissions in the real atmosphere. We have recognized this issue as a major limitation of the present study, which requires further investigations.

Page 18, Line 18 I am wondering if NMVOC and IVOC should be discussed together to implement any strategies because their sources and their effects on PM<sub>2.5</sub> and ozone could be different.

Response: We fully agree with the reviewer that the impact of NMVOC and IVOC emissions should ideally be quantified separately considering the differences in their sources and effects on SOA and O<sub>3</sub>. In the present study, they are lumped together to reduce the number of control variables in view of the fact that they have many common sources and could be controlled using similar removal technologies. To better inform NMVOC/IVOC control policies, it is needed in future studies to perform a detailed quantification of the individual contributions of NMVOC and IVOC emissions from various sources to PM<sub>2.5</sub> concentrations. We have described this limitation at the end of the revised manuscript (Page 21, Line 23-27).

Page 18, Line 24 I agree NO<sub>x</sub> reduction is necessary in the long run. However, it could increase PM<sub>2.5</sub> emissions in the near term with slight reduction. How should such adverse effects be considered? Any messages on this issue?

Response: We suggest that, in the long run, NO<sub>x</sub> emissions should be substantially reduced, preferably approach their maximum feasible reduction levels, in both the BTH and other parts of China. In the short term, we should also implement simultaneous NO<sub>x</sub> reductions in both the BTH and other regions in order to avoid the adverse effects. We have added this suggestion to the revised manuscript (Page 21, Line 4-6).

Page 18, Line 26 I feel the importance of Southern Hebei is not so discussed in the main text.

Response: We have better discussed the importance of Southern Hebei in the revised manuscript (Page 15, Line 21-27):

The precursor emissions from the northern part of BTH (e.g., Northern Hebei, Beijing) mainly contribute to local PM<sub>2.5</sub> concentrations, whereas those from the southern part of BTH (e.g., Southern Hebei) significantly affect the PM<sub>2.5</sub> concentrations in both the local region and other regions. Over the BTH, heavy pollution is frequently associated with southerly wind while strong northerly wind often blows away PM<sub>2.5</sub> pollution (Jia et al., 2008; Zheng et al., 2015), which explains the higher contribution of emissions from southern BTH to other regions.

Technical corrections

Page 6, Line 17 originally -> originally

Response: Revision has been made.

## References

- Cheng, Y. F., Zheng, G. J., Wei, C., Mu, Q., Zheng, B., Wang, Z. B., Gao, M., Zhang, Q., He, K. B., Carmichael, G., Pöschl, U., and Su, H.: Reactive nitrogen chemistry in aerosol water as a source of sulfate during haze events in China, *Sci Adv*, 2, e1601530, DOI: 10.1126/sciadv.1601530, 2016.
- Fu, X., Wang, S. X., Zhao, B., Xing, J., Cheng, Z., Liu, H., and Hao, J. M.: Emission inventory of primary pollutants and chemical speciation in 2010 for the Yangtze River Delta region, China, *Atmos Environ*, 70, 39-50, DOI 10.1016/j.atmosenv.2012.12.034, 2013.
- Fu, X., Wang, S. X., Ran, L., Pleim, J. E., Cooter, E., Bash, J. O., Benson, V., and Hao, J. M.: Estimating NH<sub>3</sub> emissions from agricultural fertilizer application in China using the bi-directional CMAQ model coupled to an agro-ecosystem model, *Atmos Chem Phys*, 15, 6637-6649, DOI 10.5194/acp-15-6637-2015, 2015.
- Fu, X., Wang, S. X., Chang, X., Cai, S. Y., Xing, J., and Hao, J. M.: Modeling analysis of secondary inorganic aerosols over China: pollution characteristics, and meteorological and dust impacts, *Sci Rep-Uk*, 6, 10.1038/srep35992, 2016.
- Gao, Y., Zhao, C., Liu, X. H., Zhang, M. G., and Leung, L. R.: WRF-Chem simulations of aerosols and anthropogenic aerosol radiative forcing in East Asia, *Atmos Environ*, 92, 250-266, DOI 10.1016/j.atmosenv.2014.04.038, 2014.
- Gordon, T. D., Presto, A. A., May, A. A., Nguyen, N. T., Lipsky, E. M., Donahue, N. M., Gutierrez, A., Zhang, M., Maddox, C., Rieger, P., Chattopadhyay, S., Maldonado, H., Maricq, M. M., and Robinson, A. L.: Secondary organic aerosol formation exceeds primary particulate matter emissions for light-duty gasoline vehicles, *Atmos Chem Phys*, 14, 4661-4678, DOI 10.5194/acp-14-4661-2014, 2014a.
- Gordon, T. D., Presto, A. A., Nguyen, N. T., Robertson, W. H., Na, K., Sahay, K. N., Zhang, M., Maddox, C., Rieger, P., Chattopadhyay, S., Maldonado, H., Maricq, M. M., and Robinson, A. L.: Secondary organic aerosol production from diesel vehicle exhaust: impact of aftertreatment, fuel chemistry and driving cycle, *Atmos Chem Phys*, 14, 4643-4659, DOI 10.5194/acp-14-4643-2014, 2014b.
- Hennigan, C. J., Miracolo, M. A., Engelhart, G. J., May, A. A., Presto, A. A., Lee, T., Sullivan, A. P., McMeeking, G. R., Coe, H., Wold, C. E., Hao, W. M., Gilman, J. B., Kuster, W. C., de Gouw, J.,

- Schichtel, B. A., Collett, J. L., Kreidenweis, S. M., and Robinson, A. L.: Chemical and physical transformations of organic aerosol from the photo-oxidation of open biomass burning emissions in an environmental chamber, *Atmos Chem Phys*, 11, 7669-7686, DOI 10.5194/acp-11-7669-2011, 2011.
- Huang, X., Song, Y., Li, M. M., Li, J. F., Huo, Q., Cai, X. H., Zhu, T., Hu, M., and Zhang, H. S.: A high-resolution ammonia emission inventory in China, *Global Biogeochem Cy*, 26, GB1030, DOI 10.1029/2011gb004161, 2012.
- Jathar, S. H., Gordon, T. D., Hennigan, C. J., Pye, H. O. T., Pouliot, G., Adams, P. J., Donahue, N. M., and Robinson, A. L.: Unspeciated organic emissions from combustion sources and their influence on the secondary organic aerosol budget in the United States, *P Natl Acad Sci USA*, 111, 10473-10478, DOI 10.1073/pnas.1323740111, 2014.
- Jia, Y. T., Rahn, K. A., He, K. B., Wen, T. X., and Wang, Y. S.: A novel technique for quantifying the regional component of urban aerosol solely from its sawtooth cycles, *J Geophys Res-Atmos*, 113, 10.1029/2008jd010389, 2008.
- Qin, Y., and Xie, S. D.: Historical estimation of carbonaceous aerosol emissions from biomass open burning in China for the period 1990-2005, *Environ Pollut*, 159, 3316-3323, DOI 10.1016/j.envpol.2011.08.042, 2011.
- Wang, G. H., Zhang, R. Y., Gomez, M. E., Yang, L. X., Zamora, M. L., Hu, M., Lin, Y., Peng, J. F., Guo, S., Meng, J. J., Li, J. J., Cheng, C. L., Hu, T. F., Ren, Y. Q., Wang, Y. S., Gao, J., Cao, J. J., An, Z. S., Zhou, W. J., Li, G. H., Wang, J. Y., Tian, P. F., Marrero-Ortiz, W., Secret, J., Du, Z. F., Zheng, J., Shang, D. J., Zeng, L. M., Shao, M., Wang, W. G., Huang, Y., Wang, Y., Zhu, Y. J., Li, Y. X., Hu, J. X., Pan, B., Cai, L., Cheng, Y. T., Ji, Y. M., Zhang, F., Rosenfeld, D., Liss, P. S., Duce, R. A., Kolb, C. E., and Molina, M. J.: Persistent sulfate formation from London Fog to Chinese haze, *P Natl Acad Sci USA*, 113, 13630-13635, 10.1073/pnas.1616540113, 2016.
- Wang, J. D., Zhao, B., Wang, S. X., Yang, F. M., Xing, J., Morawska, L., Ding, A. J., Kulmala, M., Kerminen, V. M., Kujansuu, J., Wang, Z. F., Ding, D. A., Zhang, X. Y., Wang, H. B., Tian, M., Petaja, T., Jiang, J. K., and Hao, J. M.: Particulate matter pollution over China and the effects of control policies, *Sci Total Environ*, 584, 426-447, 10.1016/j.scitotenv.2017.01.027, 2017.
- Wang, L. T., Jang, C., Zhang, Y., Wang, K., Zhang, Q. A., Streets, D., Fu, J., Lei, Y., Schreifels, J., He, K. B., Hao, J. M., Lam, Y. F., Lin, J., Meskhidze, N., Voorhees, S., Evarts, D., and Phillips, S.: Assessment of air quality benefits from national air pollution control policies in China. Part II: Evaluation of air quality predictions and air quality benefits assessment, *Atmos Environ*, 44, 3449-3457, DOI 10.1016/j.atmosenv.2010.05.058, 2010.
- Wang, S. X., and Zhang, C. Y.: Spatial and temporal distribution of air pollutant emissions from open burning of crop residues in China, *Sciencepaper Online*, 3, 1-6, 2008.
- Wang, S. X., Xing, J., Chatani, S., Hao, J. M., Klimont, Z., Cofala, J., and Amann, M.: Verification of anthropogenic emissions of China by satellite and ground observations, *Atmos Environ*, 45, 6347-6358, DOI 10.1016/j.atmosenv.2011.08.054, 2011a.
- Wang, S. X., Xing, J., Jang, C. R., Zhu, Y., Fu, J. S., and Hao, J. M.: Impact assessment of ammonia emissions on inorganic aerosols in east China using response surface modeling technique, *Environ Sci Technol*, 45, 9293-9300, DOI 10.1021/Es2022347, 2011b.
- Wang, Y., Zhang, Q. Q., He, K., Zhang, Q., and Chai, L.: Sulfate-nitrate-ammonium aerosols over China: response to 2000-2015 emission changes of sulfur dioxide, nitrogen oxides, and ammonia, *Atmos Chem Phys*, 13, 2635-2652, DOI 10.5194/acp-13-2635-2013, 2013.
- Xing, J., Wang, S. X., Jang, C., Zhu, Y., and Hao, J. M.: Nonlinear response of ozone to precursor emission changes in China: a modeling study using response surface methodology, *Atmos Chem Phys*, 11, 5027-5044, DOI 10.5194/acp-11-5027-2011, 2011.
- Zhao, B., Wang, S. X., Liu, H., Xu, J. Y., Fu, K., Klimont, Z., Hao, J. M., He, K. B., Cofala, J., and Amann, M.: NO<sub>x</sub> emissions in China: historical trends and future perspectives, *Atmos Chem Phys*, 13, 9869-9897, DOI 10.5194/acp-13-9869-2013, 2013a.

- Zhao, B., Wang, S. X., Wang, J. D., Fu, J. S., Liu, T. H., Xu, J. Y., Fu, X., and Hao, J. M.: Impact of national NO<sub>x</sub> and SO<sub>2</sub> control policies on particulate matter pollution in China, *Atmos Environ*, 77, 453-463, DOI 10.1016/j.atmosenv.2013.05.012, 2013b.
- Zhao, B., Wang, S. X., Donahue, N. M., Jathar, S. H., Huang, X. F., Wu, W. J., Hao, J. M., and Robinson, A. L.: Quantifying the effect of organic aerosol aging and intermediate-volatility emissions on regional-scale aerosol pollution in China, *Sci Rep-Uk*, 6, 10.1038/srep28815, 2016.
- Zheng, G. J., Duan, F. K., Su, H., Ma, Y. L., Cheng, Y., Zheng, B., Zhang, Q., Huang, T., Kimoto, T., Chang, D., Poschl, U., Cheng, Y. F., and He, K. B.: Exploring the severe winter haze in Beijing: the impact of synoptic weather, regional transport and heterogeneous reactions, *Atmos Chem Phys*, 15, 2969-2983, 10.5194/acp-15-2969-2015, 2015.

1 **A modeling study of the nonlinear response of fine**  
2 **particles to air pollutant emissions in the Beijing-Tianjin-**  
3 **Hebei region**

4  
5 **Bin Zhao<sup>1,2,3</sup>, Wenjing Wu<sup>1,2</sup>, Shuxiao Wang<sup>1,2</sup>, Jia Xing<sup>1,2</sup>, Xing Chang<sup>1,2</sup>, Kuo-**  
6 **Nan Liou<sup>3</sup>, Jonathan H. Jiang<sup>4</sup>, Yu Gu<sup>3</sup>, Carey Jang<sup>5</sup>, Joshua S. Fu<sup>6</sup>, Yun Zhu<sup>7</sup>,**  
7 **Jiandong Wang<sup>1,2</sup>, Jiming Hao<sup>1,2</sup>**

8 [1] School of Environment, and State Key Joint Laboratory of Environment Simulation and  
9 Pollution Control, Tsinghua University, Beijing 100084, China

10 [2] State Environmental Protection Key Laboratory of Sources and Control of Air Pollution  
11 Complex, Beijing 100084, China

12 [3] Joint Institute for Regional Earth System Science and Engineering and Department of  
13 Atmospheric and Oceanic Sciences, University of California, Los Angeles, CA 90095, USA

14 [4] Jet propulsion Laboratory, California Institute of Technology, Pasadena, CA 91109, USA

15 [5] U.S. Environmental Protection Agency, Research Triangle Park, NC 27711, USA

16 [6] Department of Civil and Environmental Engineering, University of Tennessee, Knoxville,  
17 TN 37996, United States

18 [7] School of Environmental Science and Engineering, South China University of  
19 Technology, Guangzhou 510006, China

20  
21  
22 Correspondence to: Shuxiao Wang (shxwang@tsinghua.edu.cn)

23  
24 **Abstract.**

25 The Beijing-Tianjin-Hebei (BTH) region has been suffering from the most severe fine particle  
26 (PM<sub>2.5</sub>) pollution in China, which causes serious health damage and economic loss.  
27 Quantifying the source contributions to PM<sub>2.5</sub> concentrations has been a challenging task  
28 because of the complicated non-linear relationships between PM<sub>2.5</sub> concentrations and  
29 emissions of multiple pollutants from multiple spatial regions and economic sectors. In this  
30 study, we use the Extended Response Surface Modeling (ERSM) technique to investigate the

1 nonlinear response of PM<sub>2.5</sub> concentrations to emissions of multiple pollutants from different  
2 regions and sectors over the BTH region, based on over 1000 simulations by a chemical  
3 transport model (CTM). The ERSM-predicted PM<sub>2.5</sub> concentrations agree well with  
4 independent CTM simulations, with correlation coefficients larger than 0.99 and mean  
5 normalized errors less than 1%. Using the ERSM technique, we find that, among all air  
6 pollutants, primary inorganic PM<sub>2.5</sub> makes the largest contribution (24-36%) to PM<sub>2.5</sub>  
7 concentrations. The contribution of primary inorganic PM<sub>2.5</sub> emissions is especially high in  
8 heavily polluted winter, and is dominated by the industry as well as residential and  
9 commercial sectors, which should be prioritized in PM<sub>2.5</sub> control strategies. The total  
10 contributions of all precursors (nitrogen oxides, NO<sub>x</sub>; sulfur dioxides, SO<sub>2</sub>; ammonia, NH<sub>3</sub>;  
11 non-methane volatile organic compounds, NMVOC; intermediate-volatility organic  
12 compounds, IVOC; primary organic aerosol, POA) to PM<sub>2.5</sub> concentrations range between 31%  
13 and 48%. Among these precursors, PM<sub>2.5</sub> concentrations are primarily sensitive to the  
14 emissions of NH<sub>3</sub>, NMVOC+IVOC, and POA. The sensitivities increase substantially for NH<sub>3</sub>  
15 and NO<sub>x</sub>, and decrease slightly for POA and NMVOC+IVOC with the increase in the  
16 emission reduction ratio, which illustrates the nonlinear relationships between precursor  
17 emissions and PM<sub>2.5</sub> concentrations. The contributions of primary inorganic PM<sub>2.5</sub> emissions  
18 to PM<sub>2.5</sub> concentrations are dominated by local emission sources, which account for over 75%  
19 of the total primary inorganic PM<sub>2.5</sub> contributions. For precursors, however, emissions from  
20 other regions could play similar roles as local emission sources in the summer and over the  
21 northern part of BTH. The source contribution features for various types of heavy-pollution  
22 episodes are distinctly different from each other, and from the monthly mean results,  
23 illustrating that control strategies should be differentiated based on the major contributing  
24 sources during different types of episodes.

25

## 26 **1 Introduction**

27 China is one of the regions with highest concentration of PM<sub>2.5</sub> (particulate matter with  
28 aerodynamic diameter equal to or less than 2.5 μm) in the world (van Donkelaar et al., 2015).  
29 The problem is especially serious over the Beijing-Tianjin-Hebei (BTH) region, one of the  
30 most populous and developed regions in China. Annual average PM<sub>2.5</sub> concentrations in this  
31 region reached 85-110 μg/m<sup>3</sup> during 2013-2015, which approximately triple the standard  
32 threshold (35 μg/m<sup>3</sup>) and far exceed those in other metropolitan regions (Wang et al., 2017b).

1 It has been estimated that the severe PM<sub>2.5</sub> pollution leads to about 1.05-1.23 million  
2 premature deaths per year in China (Lim et al., 2012; Burnett et al., 2014; Wang et al., 2016b),  
3 and the monetized loss over the BTH region is as high as 134 billion Chinese Yuan,  
4 representing 2.2% of regional gross domestic product (GDP) (Lv and Li, 2016). Additionally,  
5 PM<sub>2.5</sub> substantially affects global and regional climate by absorbing and scattering solar  
6 radiation and by altering cloud properties (IPCC, 2013).

7 To tackle the heavy PM<sub>2.5</sub> pollution problem, Chinese government issued the "Action Plan  
8 on Prevention and Control of Air Pollution" in September 2013, which aimed at a 25%  
9 reduction in PM<sub>2.5</sub> concentrations over the BTH region by 2017 from the 2012 levels (The  
10 State Council of the People's Republic of China, 2013). The attainment of ambient PM<sub>2.5</sub>  
11 standard would further require substantial reductions in air pollutant emissions (Wang et al.,  
12 2017b). To establish emission control strategies, many studies have apportioned the sources  
13 of PM<sub>2.5</sub> over the BTH region, either by mining monitoring data using the Positive Matrix  
14 Factorization and Chemical Mass Balance methods (e.g., Zhang et al., 2007; Yu et al., 2013)  
15 or by embedding chemical tracers in chemical transport models (CTMs) (e.g., Wang et al.,  
16 2016c; Li et al., 2015b; Ying et al., 2014). While these studies can capture the current  
17 contributions of various sources to PM<sub>2.5</sub> concentrations, these contributions could differ  
18 significantly from the PM<sub>2.5</sub> reductions induced by reducing emissions from the corresponding  
19 sources, due to highly nonlinear chemical mechanisms (Han et al., 2016; Wang et al., 2011).  
20 Therefore, it is imperative to assess the nonlinear response of PM<sub>2.5</sub> to pollutant emissions  
21 from multiple sources, which could provide direct support for the development of effective  
22 control policies.

23 The most widely used technique to evaluate the responses of PM<sub>2.5</sub> concentrations to  
24 emission changes is the "Brute force" method, which involves perturbing emissions from a  
25 certain source and repeated solution of a CTM (Russell et al., 1995). A number of studies  
26 have utilized the "Brute force" method to quantify the sensitivities of PM<sub>2.5</sub> concentrations  
27 over the BTH region to emissions from different spatial regions (Streets et al., 2007; Wang et  
28 al., 2008; Li and Han, 2016; Wang et al., 2014a) or different economic sectors (Wang et al.,  
29 2008; Han et al., 2016; Wang et al., 2014a; Liu et al., 2016), either on a seasonal basis  
30 (Streets et al., 2007; Wang et al., 2008; Han et al., 2016; Liu et al., 2016) or during a specific  
31 heavy-pollution episode (Li and Han, 2016; Wang et al., 2014a). To improve the  
32 computational efficiency, several mathematic techniques embedded in CTMs have been



1 developed to simultaneously calculate the sensitivities of the modeled concentrations to  
2 multiple emission sources, including the Decoupled Direct Method (Yang et al., 1997) and  
3 Adjoint Analysis (Sandu et al., 2005; Hakami et al., 2006). Zhang et al. (2016) used the  
4 Adjoint Analysis method to examine sensitivities of PM<sub>2.5</sub> concentrations in the BTH region  
5 to pollutant emissions during several pollution periods. However, all the preceding studies  
6 only quantified first-order sensitivities and therefore inadequately captured the nonlinearity in  
7 the responses of PM<sub>2.5</sub> concentrations to pollutant emissions, which can be extremely strong  
8 due to complex chemical mechanisms (Wang et al., 2011). Moreover, no studies have  
9 simultaneously evaluated the response of PM<sub>2.5</sub> concentrations in BTH to emissions of  
10 multiple pollutants from different sectors and regions, which we need to consider and balance  
11 to develop cost-effective control strategies.

12 In light of the drawbacks of the preceding methods, the Response Surface Modeling  
13 (RSM) technique (denoted by “conventional RSM” technique hereafter to distinguish from  
14 the ERSM technique) has been developed by using advanced statistical techniques to  
15 characterize the complex nonlinear relationship between model outputs and inputs (U.S.  
16 Environmental Protection Agency, 2006; Xing et al., 2011; Wang et al., 2011). This technique  
17 has been applied to the United States (U.S. Environmental Protection Agency, 2006) and the  
18 Eastern China (Wang et al., 2011) to evaluate the response of PM<sub>2.5</sub> and its chemical  
19 components to pollutant emissions. However, the number of emission scenarios required to  
20 build conventional RSM depends on the variable number via an equation of fourth or higher  
21 order (Zhao et al., 2015b). Therefore, the required scenario number would be tens of  
22 thousands for over 15 variables and even hundreds of thousands for over 25 variables, which  
23 is computationally impossible for most three-dimensional CTMs. To overcome this major  
24 limitation, we recently developed the Extended Response Surface Modeling (ERSM)  
25 technique (Zhao et al., 2015b), which substantially reduced the scenario number needed to  
26 build the response surface and hence extended its applicability to an increased number of  
27 regions, pollutants, and sectors with an acceptable computational burden.

28 Given the advantage of the ERSM technique, here we apply it to over 1000 simulations by  
29 the Community Multi-scale Air Quality model with Two-Dimensional Volatility Basis Set  
30 (CMAQ/2D-VBS) to systematically evaluate the nonlinear response of PM<sub>2.5</sub> to emission  
31 changes of multiple pollutants from different sectors and regions over the BTH region. The  
32 major sources contributing to PM<sub>2.5</sub> and its major components are identified and the

1 nonlinearity in the response of  $PM_{2.5}$  to emission changes is characterized. Based on results of  
2 this study, suggestions for  $PM_{2.5}$  control policies over the BTH region are proposed.

## 3 **2 Methodology**

### 4 **2.1 CMAQ/2D-VBS configuration and evaluation**

5 The CMAQ/2D-VBS model was developed in our previous study (Zhao et al., 2016) by  
6 incorporating the 2D-VBS model framework into CMAQv5.0.1. Compared with the default  
7 CMAQ, the CMAQ/2D-VBS model explicitly simulates aging of secondary organic aerosol  
8 (SOA) formed from non-methane volatile organic compounds (NMVOC), aging of primary  
9 organic aerosol (POA), and photo-oxidation of intermediate-volatility organic compounds  
10 (IVOC), thereby significantly improving the simulation results of organic aerosol (OA),  
11 particularly SOA. The model parameters within the 2D-VBS framework have been optimized  
12 in our previous studies (Zhao et al., 2015a; Zhao et al., 2016) based on a series of smog-  
13 chamber experiments. Here we use the same model parameters as those of the “High-Yield  
14 VBS” configuration reported in Zhao et al. (2016), which agrees best with surface OA and  
15 SOA observations among three model configurations. An application in the Eastern China  
16 reveals that CMAQ/2D-VBS reduces the underestimation in OA concentrations from 45%  
17 (default CMAQv5.0.1) to 19%. More importantly, while the default CMAQv5.0.1  
18 substantially underestimates the fraction of SOA in OA by 5–10 times and can not track  
19 oxygen-to-carbon ratio (O:C), the SOA fraction and O:C simulated by CMAQ/2D-VBS agree  
20 fairly well with observations.

21 We apply the CMAQ/2D-VBS model over the BTH region. One-way, double nesting  
22 simulation domains are used, as shown in Fig. 1. Domain 1 covers East Asia with a grid  
23 resolution of 36 km×36 km; domain 2 covers the BTH and its surrounding regions with a grid  
24 resolution of 12 km×12 km. We use the SAPRC99 gas-phase chemistry module and the  
25 AERO6 aerosol module, in which the treatment of OA is replaced with the 2D-VBS  
26 framework. The aerosol thermodynamics is based on ISORROPIA-II. The initial and  
27 boundary conditions for Domain 1 are kept constant as the model default profile, and those  
28 for Domain 2 are extracted from the output of Domain 1. A 5-day spin-up period is used to  
29 reduce the influence of initial conditions on modeling results.

30 The Weather Research and Forecasting Model (WRF, version 3.7) is used to generate the  
31 meteorological fields. The National Center for Environmental Prediction (NCEP)’s FNL  
32 (Final) Operational Global Analysis data (ds083.2) at  $1.0^\circ \times 1.0^\circ$  and 6-h resolution are used

1 to generate the first guess field. The NCEP's Automated Data Processing (ADP) data  
2 (ds351.0 and ds461.0) are used in objective analysis (i.e., grid nudging). The major physics  
3 options for WRF include the Kain-Fritsch cumulus scheme, the Pleim-Xiu land-surface  
4 module, the Asymmetric Convective Model with non-local upward mixing and local  
5 downward mixing (ACM2) for planetary boundary layer (PBL) parameterization, the  
6 Morrison double-moment scheme for cloud microphysics, and the Rapid Radiative Transfer  
7 Model for GCMs (RRTMG) radiation scheme. The land cover type data are obtained from the  
8 Moderate resolution Imaging Spectroradiometer (MODIS). The simulation periods are  
9 January, March, July, and October in 2014, representing winter, spring, summer, and fall. We  
10 select these four months because the occurrence frequencies of various meteorological types  
11 in these months are statistically most similar to the average conditions in winter, spring,  
12 summer, and fall during 2004-2013 (Wu, 2016).

13 A high-resolution anthropogenic emission inventory in 2014 has been developed using an  
14 "emission factor method" (Fu et al., 2013; Zhao et al., 2013b) for the BTH region by  
15 Tsinghua University. The emissions from area and mobile sources are first calculated for each  
16 prefecture-level city based on statistical data, and subsequently distributed into the model  
17 grids according to spatial distribution of population, GDP, and road networks. A unit-based  
18 method (Zhao et al., 2008) is applied to estimate and locate the emissions from large point  
19 sources (LPS) including power plants, iron and steel plants, and cement plants. The  
20 anthropogenic emission inventory in other provinces of China was originally developed for  
21 2010 and 2012 in our previous studies (Zhao et al., 2013b; Zhao et al., 2013a; Wang et al.,  
22 2014b; Cai et al., 2016), which has been updated to 2014 in this study following the same  
23 methodology. In both the BTH and national emission inventories, the emissions from open  
24 burning of agricultural residue are calculated using crop yields, straw to grain ratio, fraction  
25 of biomass burned in the open field, and emission factors (Fu et al., 2013; Zhao et al., 2013b;  
26 Wang and Zhang, 2008). We do not include the emissions from forest and grassland fires,  
27 which typically account for less than 5% of the total biomass burning emissions over the BTH  
28 region (Qin and Xie, 2011) and are not the focus of the present study. Table S1 summarizes  
29 emissions of major air pollutants in each prefecture-level city over the BTH region in 2014;  
30 Table S2 gives the provincial emissions in the whole China in 2014. The emissions for other  
31 countries are obtained from the MIX emission inventory (Li et al., 2015a) for 2010, which is  
32 the latest year available. Following our previous study (Zhao et al., 2016), we assume IVOC

1 emissions to be 30 times, 4.5 times, 1.5 times, and 3.0 times the POA emissions from gasoline  
2 vehicles, diesel vehicles, biomass burning, and other emission sources, respectively, which is  
3 based on a series of laboratory measurements (Gordon et al., 2014b; Gordon et al., 2014a;  
4 Hennigan et al., 2011; Jathar et al., 2014). The biogenic emissions were calculated by the  
5 Model of Emissions of Gases and Aerosols from Nature (MEGAN; Guenther et al., 2006).

6 We compared the simulation results of WRFv3.7 and CMAQ/2D-VBS with  
7 meteorological observations obtained from the National Climatic Data Center (NCDC), PM<sub>2.5</sub>  
8 observations at 138 state-controlled observational sites, and observations of major PM<sub>2.5</sub>  
9 chemical components at 7 sites within the modeling domain. We show that the meteorological  
10 and chemical simulations generally agree well with observations, with performance statistics  
11 mostly within the benchmark values proposed by previous studies. Details of the model  
12 evaluation methods and results are given in the Supplementary Information (Section 1, Table  
13 S3-S5, Fig. S1-S5).

## 14 **2.2 Development of ERSM prediction system**

15 The detailed methodologies of the conventional RSM and ERSM techniques have been  
16 described in our previous papers (Zhao et al., 2015b; Xing et al., 2011). Here we only  
17 summarize some key components. The conventional RSM technique characterizes the  
18 relationships between a response variable (e.g., PM<sub>2.5</sub> concentration) and a set of control  
19 variables (i.e., emissions of particular pollutants from particular sources) based on a number  
20 of randomly generated emission control scenarios (Xing et al., 2011; Wang et al., 2011). The  
21 PM<sub>2.5</sub> concentration for each emission scenario is calculated with a CTM (CMAQ/2D-VBS in  
22 this study), and the conventional RSM is subsequently established using the Maximum  
23 Likelihood Estimation - Empirical Best Linear Unbiased Predictors (MLE-EBLUPs)  
24 developed by Santner et al. (2003). Due to the limitation of the conventional RSM technique  
25 with respect to variable number, we have developed the ERSM technique (Zhao et al., 2015b)  
26 to extend the applicability to an increased number of variables and geographical regions. The  
27 ERSM technique first quantifies the relationship between PM<sub>2.5</sub> concentrations and precursor  
28 emissions for each single region using the conventional RSM technique as described above,  
29 and then assesses the effects of inter-regional transport of PM<sub>2.5</sub> and its precursors on PM<sub>2.5</sub>  
30 concentration in the target region. In order to quantify the interaction among regions, we  
31 introduce a key assumption that the emissions of precursors in the source region affect PM<sub>2.5</sub>  
32 concentrations in the target region through two major processes: (1) the inter-regional

1 transport of precursors enhancing the chemical formation of secondary PM<sub>2.5</sub> in the target  
2 region; (2) the formation of secondary PM<sub>2.5</sub> in the source region followed by transport to the  
3 target region. We quantify the individual contributions of these two processes as well as the  
4 contribution of local emissions in the target region, which are subsequently integrated to  
5 derive the total PM<sub>2.5</sub> concentrations in the target region. The development of the ERSM  
6 prediction system requires several hundred to over 1000 emission scenarios, but once built, it  
7 enables real-time prediction of PM<sub>2.5</sub> concentrations for any given control strategy and proves  
8 to be an efficient and user-friendly decision making tool. Moreover, ERSM can be applied to  
9 design least-cost control strategy once it is coupled with control cost models/functions that  
10 links the emission reductions with economic costs.

11 For application of the RSM/ERSM techniques to the BTH region, we define 5 target  
12 regions in the inner modeling domain (Domain 2), i.e., Beijing, Tianjin, Northern Hebei (N  
13 Hebei), Eastern Hebei (E Hebei), and Southern Hebei (S Hebei), as shown in Fig. 1. The  
14 decomposition of the Hebei province is based on a preliminary analysis of the pollutant  
15 transport patterns over the BTH region (Section 2 in the Supplementary Information). The  
16 simulation using back trajectory method indicates that four major types of heavy-pollution  
17 episodes in Beijing are primarily contributed by air mass from the south, the local area, the  
18 northwest, and the southeast. We develop two RSM/ERSM prediction systems (Table 1). The  
19 response variables for the first prediction system, which is built using the conventional RSM  
20 technique, are concentrations of PM<sub>2.5</sub>, SO<sub>4</sub><sup>2-</sup>, NO<sub>3</sub><sup>-</sup>, and OA over the urban areas of  
21 prefecture-level cities in the five target regions. For the second prediction system that is  
22 established using the ERSM technique, the response variables are only PM<sub>2.5</sub> concentrations.  
23 The first prediction system use 101 emission control scenarios generated by the Latin  
24 Hypercube Sample (LHS) method (Iman et al., 1980) to map atmospheric concentrations  
25 versus emissions of five PM<sub>2.5</sub> precursors, i.e., NO<sub>x</sub>, SO<sub>2</sub>, NH<sub>3</sub>, NMVOC+IVOC, and POA, in  
26 all five target regions (Table 1). It is on one hand intended for the validation of the second  
27 system (Section 3.1), and on the other hand used to study the source contributions of major  
28 PM<sub>2.5</sub> components. For the second system, the emissions of the preceding PM<sub>2.5</sub> precursors as  
29 well as primary inorganic PM<sub>2.5</sub> (i.e., the chemical components of primary PM<sub>2.5</sub> other than  
30 POA) in each of the 5 regions are categorized into 7 and 4 control variables, respectively,  
31 resulting in 55 control variables in total (Table 1). Note that we distinguish POA and primary  
32 inorganic PM<sub>2.5</sub> because the former undergoes chemical reactions and produces SOA, while

1 the latter is chemically inert in the CMAQ/2D-VBS model. We generate 1121 scenarios (see  
2 Table 1) to build the response surface, following the method detailed in Zhao et al. (2015b).  
3 Specifically, the scenarios include (1) 1 CMAQ/2D-VBS base case; (2) 200 scenarios  
4 generated by applying LHS method for the control variables of precursors in Beijing, 200×4  
5 scenarios generated in the same way for Tianjin, Northern Hebei, Eastern Hebei, and  
6 Southern Hebei; (3) 100 scenarios generated by applying LHS method for the total emissions  
7 of NO<sub>x</sub>, SO<sub>2</sub>, NH<sub>3</sub>, NMVOC+IVOC, and POA in all 5 regions; and (4) 20 scenarios where  
8 one of the control variables of primary inorganic PM<sub>2.5</sub> emissions is set to 0.25 for each  
9 scenario. Here the scenario numbers (200 in group 2 and 100 in group 3) are determined  
10 based on numerical experiments conducted in our previous studies (Xing et al., 2011; Wang et  
11 al., 2011), which showed that the response surface for 7 and 5 variables could be built with  
12 good prediction performance (mean normalized error < 1%; correlation coefficient > 0.99)  
13 using 200 and 100 scenarios, respectively. Finally, we generate 54 independent scenarios for  
14 out-of-sample validation, which will be detailed in Section. 3.1.

15 For application of the ERSM prediction system to quantitatively characterize the  
16 sensitivity of PM<sub>2.5</sub> concentrations to emission changes, we define “PM<sub>2.5</sub> sensitivity” as the  
17 change ratio of PM<sub>2.5</sub> concentration divided by the reduction ratio of a emission source,  
18 following previous studies (Zhao et al., 2015b; Wang et al., 2011).

$$19 \quad S_a^X = [(C^* - C_a) / C^*] / (1 - a) \quad (4)$$

20 where  $S_a^X$  is the PM<sub>2.5</sub> sensitivity to emission source  $X$  at its emission ratio  $a$ ;  $C^*$  and  $C_a$  are  
21 PM<sub>2.5</sub> concentrations in the base case (when the emission ratio of  $X$  is 1) and in the control  
22 scenario where the emission ratio of  $X$  is  $a$ , respectively. Similar indices can be defined for  
23 chemical components of PM<sub>2.5</sub>, such as NO<sub>3</sub><sup>-</sup>, SO<sub>4</sub><sup>2-</sup>, and OA.

24

## 25 **3 Results and discussion**

### 26 **3.1 Validation of ERSM performance**

27 The conventional RSM technique has been extensively demonstrated to have high accuracy  
28 and stability in previous papers (Xing et al., 2011; Wang et al., 2011), so we only describe the  
29 validation of the ERSM technique. Following Zhao et al. (2015b), we assess the performance  
30 of the ERSM prediction system using the “out-of-sample” and 2D-isopleths validation  
31 methods, which focus on the accuracy and stability of the prediction system, respectively.

1 For out-of-sample validation, we use the ERSM prediction system to calculate the PM<sub>2.5</sub>  
 2 concentrations for 54 “out-of-sample” control scenarios, i.e., scenarios independent from  
 3 those used to build the prediction system, and compare with the corresponding CMAQ/2D-  
 4 VBS simulation results. These 54 out-of-sample scenarios (summarized in Table S6) include  
 5 40 cases (case 1-40) where the control variables of precursors change but those of primary  
 6 inorganic PM<sub>2.5</sub> stay the same as the base case, 4 cases (case 41-44) the other way around, and  
 7 10 cases (case 45-54) where control variables of precursors and primary inorganic PM<sub>2.5</sub>  
 8 change simultaneously. Most cases are generated randomly with the LHS method (case 4-6,  
 9 10-12, 16-18, 22-24, 28-54), and some cases are designed where all control variables are  
 10 subject to large emission changes (case 1-3, 7-9, 13-15, 19-21, 25-27).

11 Figure 2 compares the ERSM-predicted and CMAQ/2D-VBS-simulated PM<sub>2.5</sub>  
 12 concentrations and PM<sub>2.5</sub> responses (defined as the difference between PM<sub>2.5</sub> concentration in  
 13 an emission control scenario and that in the base case) for the out-of-sample scenarios using  
 14 scatter plots. Table 2 summarizes the statistics of the model performance. The definitions of  
 15 normalized error (NE), mean normalized error (MNE), and normalized mean error (NME) are  
 16 given as follows:

$$17 \quad \text{NE} = |P_i - S_i| / S_i \quad (1)$$

$$18 \quad \text{MNE} = \frac{1}{N_s} \sum_{i=1}^{N_s} [|P_i - S_i| / S_i] \quad (2)$$

$$19 \quad \text{NME} = \sum_{i=1}^{N_s} |P_i - S_i| / \sum_{i=1}^{N_s} S_i \quad (3)$$

20 where  $P_i$  and  $S_i$  are the ERSM-predicted and CMAQ/2D-VBS-simulated value of the  $i^{\text{th}}$  out-  
 21 of-sample scenario;  $N_s$  is the number of out-of-sample scenarios. Figure 2 shows that the  
 22 ERSM predictions and CMAQ/2D-VBS simulations agree well with each other. For PM<sub>2.5</sub>  
 23 concentrations, the correlation coefficients are larger than 0.99, and the MNEs and NMEs are  
 24 less than 1% for all four months. The maximum NEs could be as large as 11% for particular  
 25 month and region, but the 95% percentiles of NEs are all within 4.4%. NEs exceeding 4.4%  
 26 happen only for the scenarios where most control variables are reduced substantially,  
 27 indicating relatively large errors at low emission rates, which is consistent with our previous  
 28 study (Zhao et al., 2015b). Note that all sensitivity scenarios used in Sections 3.2-3.4 have  $\leq$   
 29 80% emission reductions, which helps to avoid relatively large errors. We also examine the  
 30 errors in predicted PM<sub>2.5</sub> response. Since the CMAQ/2D-VBS-simulated PM<sub>2.5</sub> responses are  
 31 very close to zero in several scenarios, their normalized errors (NEs) and mean normalized  
 32 errors (MNEs) could be extremely large even if the absolute errors are small, which cannot

1 properly characterize the accuracy of the ERSM technique. For this reason, we only calculate  
2 the correlation coefficients and NMEs (Table 2). The correlation coefficients of PM<sub>2.5</sub>  
3 response are larger than 0.99, and the NMEs are within 5.6% for all months. In summary, the  
4 out-of-sample validation indicates an overall good agreement between ERSM predictions and  
5 CMAQ/2D-VBS simulations.

6 We further examine whether the ERSM technique can capture the trends in PM<sub>2.5</sub>  
7 concentrations in response to continuous changes in precursor emissions, i.e., the stability of  
8 the ERSM technique. To this end, we compare the 2D-isopleths of PM<sub>2.5</sub> concentrations as a  
9 function of simultaneous changes in two precursors' emissions in all five regions derived  
10 from the ERSM and conventional RSM techniques. It should be noted that, although the  
11 ERSM technique is applicable to a much larger number of control variables than conventional  
12 RSM, the assumptions in the treatment of inter-regional transport (Section 2.2) in ERSM  
13 might affect its accuracy. Nevertheless, the predictions by conventional RSM can be regarded  
14 as proxies for real CMAQ/2D-VBS simulations since it has been extensively demonstrated to  
15 have high accuracy and stability in previous studies (Xing et al., 2011; Wang et al., 2011). For  
16 this reason, the comparison between the ERSM and conventional RSM techniques helps to  
17 evaluate the stability of the ERSM technique. Figure 3 illustrates the PM<sub>2.5</sub> isopleths in  
18 Beijing as a function of three combinations of precursors, i.e., NO<sub>x</sub> vs NH<sub>3</sub>, SO<sub>2</sub> vs NH<sub>3</sub>, and  
19 VOC+IVOC vs POA; the isopleths for other regions are very similar and thus not shown. The  
20 X- and Y-axis of the figures represent the "emission ratio", defined as the ratios of the  
21 changed emissions to the emissions in the base case. For example, an emission ratio of 0.7  
22 means the emission of a particular control variable accounts for 70% that of the base case.  
23 The colour isopleths represent PM<sub>2.5</sub> concentrations. The comparison shows that the shapes of  
24 isopleths derived from both prediction systems generally agree with each other. The  
25 agreement is very good for the case of VOC+IVOC vs POA, and for the cases of NO<sub>x</sub> vs NH<sub>3</sub>  
26 and SO<sub>2</sub> vs NH<sub>3</sub> when the emission ratios for NO<sub>x</sub> and NH<sub>3</sub> are larger than 0.2. Relatively  
27 large errors occur at very low NO<sub>x</sub>/NH<sub>3</sub> emission ratios (< 0.2) due primarily to an extremely  
28 strong nonlinearity. Within these low emission ranges, the ERSM technique can capture the  
29 general trends in PM<sub>2.5</sub> concentrations in response to emission changes, but the concentration  
30 gradients predicted by ERSM are smaller than those given by conventional RSM. More  
31 studies are needed to further improve the performance of ERSM at very low NO<sub>x</sub>/NH<sub>3</sub>  
32 emission ratios. Despite the existing errors, the general consistency between RSM and



1 ERSM-predicted isopleths demonstrates the stability of the ERSM prediction system. In other  
2 words, the discrepancies between ERSM and CMAQ/2D-VBS cannot challenge the major  
3 conclusions on the effectiveness of emission reductions. Finally, as stated in the last  
4 paragraph, all sensitivity scenarios used in the following discussions have emission ratios  $\geq$   
5 0.2, since  $< 0.2$  emission reductions are quite rare as limited by the technologically feasible  
6 reduction potentials (Wang et al., 2014b).

### 7 **3.2 Response of PM<sub>2.5</sub> concentrations to emissions of air pollutants**

8 Having demonstrated the reliability of the ERSM prediction system, we employ it to  
9 investigate the responses of PM<sub>2.5</sub> concentrations to emissions of various pollutants from  
10 different sectors and regions. We use “PM<sub>2.5</sub> sensitivity” defined in Section 2.2 to  
11 quantitatively characterize the sensitivity of PM<sub>2.5</sub> concentrations to emission changes. Figure  
12 4 illustrates the sensitivity of 4-month (January, March, July, and October) mean PM<sub>2.5</sub>  
13 concentrations to stepped control of individual air pollutants (left panel) and individual  
14 pollutant-sector combinations (right panel) in the BTH region, which are derived from the  
15 ERSM technique. The left panel of Fig. 4 can be obtained from both the RSM and ERSM  
16 prediction systems and their results are consistent, whereas the right panel of Fig. 4, as well as  
17 the results shown in Fig. 5 and 6 can only be derived from ERSM. Among all pollutants, the  
18 4-month mean PM<sub>2.5</sub> concentrations are most sensitive to the emissions of primary inorganic  
19 PM<sub>2.5</sub> in all five regions, and the PM<sub>2.5</sub> sensitivities vary from 24% to 36% according to  
20 region. When primary inorganic PM<sub>2.5</sub> emissions from various sectors are differentiated, the  
21 industry sector is found to make the largest contribution to PM<sub>2.5</sub> concentrations, followed by  
22 the residential and commercial sectors; the contribution of power plants is negligibly small  
23 because of smaller emissions and higher stacks. The PM<sub>2.5</sub> sensitivities to primarily inorganic  
24 PM<sub>2.5</sub> emissions remain constant at various reduction ratios.

25 While primary inorganic PM<sub>2.5</sub> makes the largest contribution to PM<sub>2.5</sub> concentrations  
26 among all air pollutants, the total contributions of all precursors (NO<sub>x</sub>, SO<sub>2</sub>, NH<sub>3</sub>, NMVOC,  
27 IVOC, and POA), which range between 31% and 48%, exceed that of primary inorganic  
28 PM<sub>2.5</sub> (24-36%). Among the precursors, PM<sub>2.5</sub> concentrations are primarily sensitive to the  
29 emissions of NH<sub>3</sub>, NMVOC+IVOC, and POA, and their relative importance differ according  
30 to reduction ratio. The PM<sub>2.5</sub> sensitivity to NH<sub>3</sub> increases substantially with the increase of  
31 reduction ratio, primarily attributable to the transition from NH<sub>3</sub>-rich to NH<sub>3</sub>-poor regimes  
32 when more controls are enforced. The PM<sub>2.5</sub> sensitivities to POA and NMVOC+IVOC,

1 however, decrease slightly with the increase of reduction ratio. This is because that, based on  
2 the gas-particle absorptive partitioning theory, organics have a higher tendency to partition  
3 into the particle phase at larger OA concentrations. As a result of the nonlinearity, the PM<sub>2.5</sub>  
4 sensitivities to POA and NMVOC+IVOC emissions are larger than those to NH<sub>3</sub> emissions at  
5 small reduction ratios (e.g., 20%), while it is the other way around at large reduction ratios  
6 (e.g., 80%).

7 The PM<sub>2.5</sub> sensitivity to SO<sub>2</sub> emissions is considerably smaller compared with the three  
8 precursors above, and does not change significantly as a function of reduction ratio. From  
9 2007 to 2014 (the base year of this study), both SO<sub>2</sub> emissions and SO<sub>4</sub><sup>2-</sup> concentrations in  
10 PM<sub>2.5</sub> have been continuously decreasing due to effective control policies (Wang et al., 2017a),  
11 which partly explains the small sensitivity of PM<sub>2.5</sub> to SO<sub>2</sub> emissions. The response of PM<sub>2.5</sub>  
12 concentrations to NO<sub>x</sub> emissions could change from negative to positive with the increase of  
13 reduction ratio, which has been reported in several previous studies (Dong et al., 2014; Zhao  
14 et al., 2013c; Cai et al., 2016). Small NO<sub>x</sub> emission reductions could lead to increase in O<sub>3</sub>  
15 and HO<sub>x</sub> concentrations in several seasons owing to a NMVOC-limited photochemical  
16 regime, which on one hand enhances SO<sub>4</sub><sup>2-</sup> and SOA formation, and on the other hand, could  
17 also increase NO<sub>3</sub><sup>-</sup> concentrations by accelerating the nocturnal formation of N<sub>2</sub>O<sub>5</sub> and HNO<sub>3</sub>  
18 through the NO<sub>2</sub> + O<sub>3</sub> reaction at low temperatures. A substantial reduction in NO<sub>x</sub> emissions,  
19 however, transforms the NMVOC-limited regime to a NO<sub>x</sub>-limited regime, resulting in a  
20 successive decline in concentrations of O<sub>3</sub>, HO<sub>x</sub>, and most PM<sub>2.5</sub> chemical components.  
21 Judging from the our simulation results (Fig. 4), if only the NO<sub>x</sub> emissions within the BTH  
22 region are controlled, a very large reduction ratio of about 80% is required to realize a  
23 reduction in annual PM<sub>2.5</sub> concentrations in most areas. However, the effects could be  
24 distinctly different if NO<sub>x</sub> emissions outside the BTH region are jointly reduced. Our  
25 previous studies using the CMAQ model (Zhao et al., 2013c; Wang et al., 2010; Wang et al.,  
26 2011) have shown that uniform reductions in NO<sub>x</sub> emissions in the whole China by 23-50%  
27 result in considerable annual PM<sub>2.5</sub> reduction over the BTH region. This is because NO<sub>x</sub>  
28 emission reductions in upwind regions are more likely to result in a net PM<sub>2.5</sub> decrease  
29 compared with local emission reductions, since the photochemistry typically changes from a  
30 NMVOC-limited regime in local urban areas at surface to a NO<sub>x</sub>-limited regime in downwind  
31 areas or at upper levels (Xing et al., 2011). The results shown in Fig. 4 also support the above-  
32 mentioned pattern and mechanism to some extent: even a 20% NO<sub>x</sub> emission reduction in

1 BTH can lead to  $PM_{2.5}$  decrease in Northern Hebei, because, as the northernmost region in  
2 BTH, it is significantly affected by emissions in other regions within BTH. Note that some  
3 recently discovered chemical pathways are missing in the model, such as the oxidation of  $SO_2$   
4 by  $NO_2$  in aerosol water and the  $SO_2$  heterogeneous reactions on the dust surface (Fu et al.,  
5 2016; Cheng et al., 2016; Wang et al., 2016a). Incorporation of these processes in the model  
6 may affect the simulated responses of  $PM_{2.5}$  to  $NO_x$  and  $SO_2$  emissions. Regarding emission  
7 sectors, the contributions of  $SO_2$  and  $NO_x$  emissions are dominated by “other sources” (sources  
8 other than LPS) because they emit larger amount of pollutants at lower height compared with  
9 LPS.

10 The black dotted lines in Fig. 4 show the  $PM_{2.5}$  sensitivity when all pollutants from all  
11 sectors are controlled simultaneously. The sum of  $PM_{2.5}$  sensitivities to individual pollutant-  
12 sector combinations (stacked columns) is mostly larger than the sensitivity to all pollutants  
13 and sectors (black dotted lines), especially under large reduction ratios. This is mainly  
14 attributed to the overlapping effect of two precursors (e.g.,  $SO_2$  and  $NH_3$ ) involved in the  
15 formation of ammonium sulfate and ammonium nitrate. Nevertheless, at small reduction  
16 ratios, the sum of individual sensitivities is sometimes smaller, because the negative effects of  
17 reducing  $NO_x$  are mitigated when we simultaneously reduce  $NO_x$  emissions from multiple  
18 sectors as well as emissions of other air pollutants such as NMVOC. When all pollutants and  
19 sectors are controlled together, the  $PM_{2.5}$  sensitivity generally increases with reduction ratio,  
20 indicating that additional air quality benefit could be achieved, larger than the expectation  
21 from linear extrapolation, if more control measures are implemented.

22 Figure 5 illustrates the  $PM_{2.5}$  sensitivities to individual pollutant-sector combinations in  
23 each month. The source contribution features are significantly discrepant in different months.  
24 The contributions of primary inorganic  $PM_{2.5}$  emissions to  $PM_{2.5}$  concentrations are notably  
25 higher in January than in other months, which is probably attributed to weaker dilution and  
26 slower chemical reactions in January. Regarding different emission sectors of primary  
27 inorganic  $PM_{2.5}$ , the industrial sector plays a dominant role in all months except January,  
28 when the residential and commercial sectors make a similar or even larger contribution as  
29 compared to the industrial sector. The higher contribution of the residential and commercial  
30 sectors in January is on one hand because of the higher emissions due to heating, and on the  
31 other hand explained by weaker vertical mixing in winter, which results in a larger relative  
32 contribution of low-level sources. This result highlights the importance of residential and

1 commercial sources for PM<sub>2.5</sub> pollution controls in the winter. The contributions of precursors  
2 are dominated by POA and NMVOC+IVOC in January, while in July, NO<sub>x</sub>, SO<sub>2</sub>, and NH<sub>3</sub>,  
3 which are known to be precursors of secondary inorganic aerosols, make larger contributions  
4 than POA and NMVOC+IVOC. The responses of PM<sub>2.5</sub> concentrations to NO<sub>x</sub> emissions can  
5 be opposite in different seasons. Specifically, in July, NO<sub>x</sub> emission reductions always induce  
6 decrease in PM<sub>2.5</sub> concentrations due to a NO<sub>x</sub>-limited photochemical regime. In January,  
7 however, even a 80% reduction in NO<sub>x</sub> emissions (roughly the maximum technically feasible  
8 reduction ratio) could result in a net PM<sub>2.5</sub> increase, as a result of a strong NMVOC-limited  
9 regime. To achieve a net PM<sub>2.5</sub> reduction in January, it would be necessary to simultaneously  
10 reduce NO<sub>x</sub> emissions outside the BTH region.

11 We further evaluate the contributions of primary inorganic PM<sub>2.5</sub> and precursor emissions  
12 from various regions to PM<sub>2.5</sub> concentrations (Fig. 6, Fig. S6). Here the contributions are  
13 quantified by comparing the base case with sensitivity scenarios in which emissions from a  
14 specific source are reduced by 80%, which reaches the maximum technologically feasible  
15 reduction ratios of major pollutants in most areas (Wang et al., 2014b). Obviously, the  
16 contributions of total primary inorganic PM<sub>2.5</sub> emissions in the BTH region are dominated by  
17 local sources, which account for over 75% of the total primary inorganic PM<sub>2.5</sub> contributions.  
18 When precursor emissions are decomposed into different regions, local sources usually also  
19 represent the largest contributors, but precursor emissions from other regions (denoted by  
20 “regional precursor emissions” hereafter) could also make significant contributions,  
21 depending on regions and seasons. The precursor emissions from the northern part of BTH  
22 (e.g., Northern Hebei, Beijing) mainly contribute to local PM<sub>2.5</sub> concentrations, whereas those  
23 from the southern part of BTH (e.g., Southern Hebei) significantly affect the PM<sub>2.5</sub>  
24 concentrations in both the local region and other regions. Over the BTH, heavy pollution is  
25 frequently associated with southerly wind while strong northerly wind often blows away  
26 PM<sub>2.5</sub> pollution (Jia et al., 2008; Zheng et al., 2015), which explains the higher contribution of  
27 emissions from southern BTH to other regions. Moreover, the importance of regional  
28 precursor emissions relative to local ones is remarkably higher in July than in January, which  
29 can be explained by the southerly monsoon and stronger vertical mixing in summer that  
30 favors inter-regional transport of air pollutants. We also examine the contributions of  
31 emissions outside the BTH region to PM<sub>2.5</sub> concentrations in the five target regions. The  
32 results reveal that these emissions contribute 24-33% of the 4-month mean PM<sub>2.5</sub>

1 concentrations, among which more than 80% could be attributed to precursor emissions.  
2 Among the four months, the contribution of emissions outside BTH is considerably smaller in  
3 January (12-21%) as compared to other months (29-38%).

### 4 **3.3 Response of PM<sub>2.5</sub> chemical components to emissions of air pollutants**

5 Ambient PM<sub>2.5</sub> is comprised of complicated chemical components with distinctly different  
6 formation pathways. To gain deeper insight into the formation mechanisms and source  
7 attribution of PM<sub>2.5</sub>, we examine the sensitivities of major PM<sub>2.5</sub> components, including NO<sub>3</sub><sup>-</sup>,  
8 SO<sub>4</sub><sup>2-</sup>, and OA, to stepped control of individual air pollutants, as shown in Fig. 7 (January and  
9 July) and Fig. S7 (March and October). NO<sub>3</sub><sup>-</sup> concentrations are most sensitive to NH<sub>3</sub>  
10 emissions in all months except July, when the sensitivities of NO<sub>3</sub><sup>-</sup> concentrations to NH<sub>3</sub> and  
11 NO<sub>x</sub> emissions are similar. The NO<sub>3</sub><sup>-</sup> sensitivities to NO<sub>x</sub> emissions differ significantly  
12 according to season. In most months, NO<sub>3</sub><sup>-</sup> concentrations are positively correlated with NO<sub>x</sub>  
13 emissions. In January, however, the sensitivities of NO<sub>3</sub><sup>-</sup> concentrations to NO<sub>x</sub> emissions are  
14 mostly negative and could be positive at large reduction ratios, which can be explained by a  
15 very strong NMVOC-limited photochemical regime, and abundant ice water for  
16 heterogeneous formation of HNO<sub>3</sub> from N<sub>2</sub>O<sub>5</sub> at cold temperatures. The sensitivities of NO<sub>3</sub><sup>-</sup> to  
17 both NH<sub>3</sub> and NO<sub>x</sub> emissions show pronounced increasing trends with the increase of  
18 reduction ratio, in agreement with the strong nonlinearity in these two pollutants described in  
19 Section 3.2. NMVOC emissions make moderate positive contributions to NO<sub>3</sub><sup>-</sup>, with the  
20 largest and smallest contributions occurring in January and July in conjunction with NMVOC-  
21 limited and NO<sub>x</sub>-limited photochemical regimes, respectively. Finally, SO<sub>2</sub> emissions have  
22 very small influences on NO<sub>3</sub><sup>-</sup> concentrations.

23 For SO<sub>4</sub><sup>2-</sup>, SO<sub>2</sub> emissions represent the dominant contributor in all months. The sensitivity  
24 of SO<sub>4</sub><sup>2-</sup> concentrations to SO<sub>2</sub> emissions does not change significantly with respect to  
25 reduction ratio, consistent with the results shown in Section 3.2. The contributions of NH<sub>3</sub>  
26 emissions to SO<sub>4</sub><sup>2-</sup> concentrations are quite small except in October, when NH<sub>3</sub> accounts for  
27 approximately one fourth the contribution of SO<sub>2</sub>. NO<sub>x</sub> emissions affect SO<sub>4</sub><sup>2-</sup> concentrations  
28 mainly by altering O<sub>3</sub> and HO<sub>x</sub> concentrations, the effects of which are positive in July at  
29 large reduction ratios, and mostly negative in other months. NMVOC emissions can impose  
30 small impact on SO<sub>4</sub><sup>2-</sup> concentrations primarily through changing O<sub>3</sub> and HO<sub>x</sub> concentrations.

31 The emissions of POA and NMVOC+IVOC are obviously two major contributors to OA  
32 concentrations. The relative importance of the two is strongly dependent on season. In July,

1 POA and NMVOC+IVOC make similar contributions to OA concentrations, while POA  
2 usually contributes more in other months. In January, the contribution of POA could account  
3 for about four times those of NMVOC+IVOC. The higher relative contribution of POA  
4 emissions in January can be explained by several reasons. First, the POA emissions are  
5 relatively higher in January due to residential heating, while the NMVOC emissions from  
6 solvent use and biogenic sources are higher in July. Second, lower temperature in winter  
7 favors the partitioning of the semi-volatile components comprising POA to the particle phase,  
8 whereas higher temperature and stronger radiation in July accelerate the formation of SOA  
9 from NMVOC+IVOC. Similar to  $\text{SO}_4^{2-}$ , the impact of  $\text{NO}_x$  emissions on OA concentrations  
10 also works through two pathways. Besides the abovementioned photochemical pathway,  $\text{NO}_x$   
11 emission reductions could lead to OA increases due to the fact that SOA yield, defined as the  
12 ratio of SOA formation to the consumption of a precursor, is generally higher at a low- $\text{NO}_x$   
13 condition than at a high- $\text{NO}_x$  condition. As an integrated effect, the responses of OA  
14 concentrations to  $\text{NO}_x$  emissions are negative in most situations.

### 15 **3.4 $\text{PM}_{2.5}$ responses to emission reductions during heavy-pollution episodes**

16 Having shown the responses of monthly-mean  $\text{PM}_{2.5}$  concentrations to pollutant emissions,  
17 we are also interested in heavy-pollution episodes, in which the source contributions could be  
18 quite different from the monthly-mean results, largely due to variations in meteorological  
19 conditions. To provide more insight into the control strategies for heavy pollution, we use the  
20 ERSM technique to investigate the source contribution features during three typical heavy-  
21 pollution episodes. We first select 47 heavy-pollution episodes over the BTH region during  
22 2013-2015 (Table S7). Subsequently, we employ the Hybrid Single Particle Lagrangian  
23 Integrated Trajectory (HYSPLIT) model (Stein et al., 2015) and Concentration Weighted  
24 Trajectory (CWT) method (Cheng et al., 2013) to identify the potential source regions for  
25  $\text{PM}_{2.5}$  during each episode, and categorize these episodes according to their source regions.  
26 We then select a representative episode from each of three most important pollution types in  
27 which the air mass primarily originates from local areas (“Local” type), from the south  
28 (“South” type), and from the southeast (“Southeast” type). We give preference to episodes  
29 within the four-month simulation period of this study to facilitate a comparison with the  
30 monthly-mean source contribution features. For this reason, we select (1) January 5-7, 2014,  
31 (2) October 7-11, 2014, and (3) October 29-31, 2014 as representatives of the “Local”,

1 “South”, and “Southeast” types. The selection of heavy-pollution episodes is detailed in  
2 Section 2 of the Supplementary Information.

3 Figure 8 shows the contribution of precursor and primary inorganic PM<sub>2.5</sub> emissions from  
4 individual regions to PM<sub>2.5</sub> concentrations during the three heavy-pollution episodes, and Fig.  
5 9 illustrates the sensitivity of PM<sub>2.5</sub> concentrations to stepped control of individual pollutant-  
6 sector combinations. During January 5-7, 2014 (“Local” type), the contributions of local  
7 emission sources to PM<sub>2.5</sub> concentrations far exceed those from other regions within BTH as  
8 well as from outside of BTH (Fig. 8). In contrast to the monthly mean results (Section 3.2),  
9 the contributions of primary inorganic PM<sub>2.5</sub> emissions are comparable to, and even larger  
10 than those of precursor emissions in the BTH region. The total contributions of primary PM<sub>2.5</sub>  
11 (including POA) account for as high as 70-80% of the contributions of all pollutants within  
12 the BTH region, which highlights the crucial importance of primary PM<sub>2.5</sub> controls during this  
13 episode. Moreover, the controls of NMVOC, NH<sub>3</sub>, and SO<sub>2</sub> emissions could contribute  
14 moderately to reducing PM<sub>2.5</sub> concentrations. However, NO<sub>x</sub> emission reduction induces an  
15 increase in PM<sub>2.5</sub> concentrations, even at an 80% reduction ratio. Therefore, effective  
16 temporary control measures for this episode should focus on the controls of local emissions,  
17 with emphasis laid on primary PM<sub>2.5</sub>.

18 During October 7-11, 2014 (“South” type), the contributions of emissions outside BTH to  
19 PM<sub>2.5</sub> concentrations are as large as 33% in Beijing, and 40-50% in other regions. Within the  
20 BTH region, the emissions from Southern Hebei can have similar effects to local emissions  
21 on PM<sub>2.5</sub> concentrations in Beijing, indicating a strong long-range transport from the south. In  
22 addition, the total contributions of precursor emissions about double those of primary  
23 inorganic PM<sub>2.5</sub> emissions. Among all precursors, PM<sub>2.5</sub> concentrations are mainly sensitive to  
24 emissions of NH<sub>3</sub>, NMVOC+IVOC, and POA. The sensitivity of PM<sub>2.5</sub> concentrations to NO<sub>x</sub>  
25 emissions increases dramatically with reduction ratio. Although small NO<sub>x</sub> reductions may  
26 slightly elevate PM<sub>2.5</sub> concentrations, large NO<sub>x</sub> emission reduction (> 50%) can result in  
27 significant PM<sub>2.5</sub> reduction. To effectively mitigate PM<sub>2.5</sub> pollution during this episode, we  
28 should implement control measures for precursor emissions in both the BTH region  
29 (especially the southern part) and regions south of BTH. The NO<sub>x</sub> emissions, if controlled,  
30 should be reduced by at least 50% to avoid adverse side effect.

31 For October 29-31, 2014 (“Southeast” type), PM<sub>2.5</sub> concentrations are also significantly  
32 affected by emissions outside the BTH region. Within the BTH region, the PM<sub>2.5</sub>

1 concentrations in Beijing and Northern Hebei are about equally affected by local emissions  
2 and emissions from Eastern Hebei and Southern Hebei, while local emissions play dominant  
3 roles in other regions. The emissions of both precursor and primary inorganic  $PM_{2.5}$  within the  
4 BTH region make important contributions to  $PM_{2.5}$  concentrations, and the relative  
5 significance of the two is dependent on region. All precursors except  $NO_X$  can contribute  
6 considerably to  $PM_{2.5}$  reductions, and the sensitivity of  $PM_{2.5}$  to  $NH_3$  increase rapidly with  
7 emission ratio.  $NO_X$  emissions are negatively correlated with  $PM_{2.5}$  concentrations in most  
8 cases. Regarding the temporary control strategy for this episode, it is preferable to implement  
9 joint controls of primary  $PM_{2.5}$  and precursors both within and outside the BTH region, with  
10 stringent measures over the Eastern and Southern Hebei.

11 From the analysis above, we conclude that the source contributions are tremendously  
12 different in these three episodes, which have been demonstrated to represent some key  
13 features of the corresponding pollution types (“Local”, “South”, and “Southeast” types).  
14 Therefore, episode-specific control strategies need to be formulated based on the source  
15 contribution features of individual pollution types. Nevertheless, the results of this study are  
16 not yet sufficient to guide the development of temporary control strategies for all heavy-  
17 pollution episodes, because the conclusions drawn from the three episodes may not be  
18 generalized to pollution types. In future studies, we need to simulate more episodes to  
19 improve their classification and to comprehensively understand the source contribution  
20 features of each pollution type. For a coming heavy-pollution episode, we can predict its  
21 pollution type using an air quality forecasting model, and subsequently formulate the  
22 temporary control strategies based on the source contribution features of this specific  
23 pollution type.

#### 24 **4 Conclusion and implications**

25 In the present study, we investigated the nonlinear response of  $PM_{2.5}$  concentrations to  
26 emission changes of multiple pollutants from different sectors and regions over the BTH  
27 region, using the ERSM technique coupled with the CMAQ/2D-VBS model.

28 Among all pollutants, primary inorganic  $PM_{2.5}$  makes the largest contribution (24-36%) to  
29 the 4-month mean  $PM_{2.5}$  concentrations. The contribution from primary inorganic  $PM_{2.5}$  is  
30 especially high in heavily polluted winter, and is dominated by the industry as well as  
31 residential and commercial sectors. The total contributions of all precursors to  $PM_{2.5}$   
32 concentrations range between 31% and 48%. Among the precursors,  $PM_{2.5}$  concentrations are



1 primarily sensitive to the emissions of  $\text{NH}_3$ , NMVOC+IVOC, and POA. With the increase of  
2 reduction ratio, the sensitivities of  $\text{PM}_{2.5}$  concentrations to pollutant emissions remain roughly  
3 constant for primary inorganic  $\text{PM}_{2.5}$  and  $\text{SO}_2$ , increase substantially for  $\text{NH}_3$  and  $\text{NO}_x$ , and  
4 decrease slightly for POA and NMVOC+IVOC. The contributions of primary inorganic  $\text{PM}_{2.5}$   
5 emissions to  $\text{PM}_{2.5}$  concentrations are dominated by local emission sources, which account for  
6 over 75% of the total primary inorganic  $\text{PM}_{2.5}$  contributions. For precursors, however,  
7 emissions from other regions could play similar roles to local emission sources in the summer  
8 and over the northern part of BTH. Different  $\text{PM}_{2.5}$  chemical components are associated with  
9 distinct source contribution features. The  $\text{NO}_3^-$  and  $\text{SO}_4^{2-}$  concentrations are most sensitive to  
10 emissions of  $\text{NH}_3$  and  $\text{SO}_2$ , respectively. The emissions of the POA and NMVOC+IVOC are  
11 two major contributors to OA concentrations, with their relative importance depending on  
12 season.

13 The source contribution features are significantly different for three typical heavy-  
14 pollution episodes, which belong to three distinct pollution types. The  $\text{PM}_{2.5}$  concentrations in  
15 the first episode (“Local” type) are dominated by local sources and primary  $\text{PM}_{2.5}$  emissions,  
16 while the second episode (“South” type) is primarily affected by precursor emissions from  
17 local and southern regions. The third episode (“Southeast” type) is significantly influenced by  
18 emissions of both primary inorganic  $\text{PM}_{2.5}$  and precursors from multiple regions. Future  
19 investigations are needed to acquire generalized patterns for the source contributions of  
20 various heavy-pollution types.

21 The results of the present study have important implications for  $\text{PM}_{2.5}$  control policies  
22 over the BTH region. First, the controls of primary  $\text{PM}_{2.5}$  emissions should be a priority in  
23  $\text{PM}_{2.5}$  control strategies. Primary  $\text{PM}_{2.5}$ , including primary inorganic  $\text{PM}_{2.5}$  and POA,  
24 contribute over half of the 4-month mean  $\text{PM}_{2.5}$  concentrations, which is even higher in the  
25 winter when heavy pollution frequently occurs. The industry sector and the residential and  
26 commercial sectors represent 85% of the total primary  $\text{PM}_{2.5}$  emissions, and therefore should  
27 be the focus of primary  $\text{PM}_{2.5}$  controls. In particular, we should pay special attention to the  
28 residential and commercial sectors, which account for half of the total contribution of primary  
29  $\text{PM}_{2.5}$  emissions to  $\text{PM}_{2.5}$  concentrations in the winter but have been frequently neglected in  
30 China’s previous control policies. Second, the control policies for NMVOC and IVOC  
31 emissions should be strengthened. The sensitivity of  $\text{PM}_{2.5}$  concentrations to NMVOC+IVOC  
32 is one of the largest among all precursors. In particular, the controls of NMVOC and IVOC

1 emissions are very effective for PM<sub>2.5</sub> reduction even at the initial control stage, as indicated  
2 by the large sensitivity at small reduction ratios. Moreover, NMVOC reduction is also crucial  
3 for the mitigation of O<sub>3</sub> pollution considering a NMVOC-limited regime over the urban and  
4 its surrounding areas (Xing et al., 2011). Third, NO<sub>x</sub> emissions should be substantially  
5 reduced in both the BTH and other parts of China; in the long run, the reduction ratio should  
6 preferably approach their maximum feasible reduction levels. Fourth, more stringent control  
7 policies should be enforced in Southern Hebei, which on one hand suffers from the most  
8 severe PM<sub>2.5</sub> pollution (Wang et al., 2014a), and on the other hand, significantly affects both  
9 local and regional PM<sub>2.5</sub> concentrations. Last but not least, considering the distinct source  
10 contributions in different heavy pollution episodes, episode-specific temporary control  
11 strategies should be formulated according to the source contribution feature of the specific  
12 pollution type.

13 The present study has a few limitations. First, the establishment of ERSM requires several  
14 hundred or over 1000 emission scenarios, although the scenario number needed for a specific  
15 number of control variables has already been dramatically reduced as compared to the  
16 conventional RSM technique. Studies are needed to further reduce the scenario number but  
17 retain the accuracy of the ERSM technique. Second, the current ERSM technique has not  
18 considered the impact of meteorological variations on ambient concentrations. Third,  
19 although the responses of PM<sub>2.5</sub> concentrations to precursor emissions predicted by ERSM  
20 have been demonstrated to agree well with chemical transport model simulations, evaluating  
21 the predicted responses against the actual situation in the real atmosphere still represents a  
22 major challenge, because it is extremely difficult to artificially perturb emissions in the  
23 atmosphere. Last but not the least, the NMVOC and IVOC emissions have been lumped  
24 together in this study to reduce the number of control variables. Considering their differences  
25 in sources and SOA formation potentials, a detailed quantification of the individual  
26 contributions of NMVOC and IVOC emissions from various sources to PM<sub>2.5</sub> concentrations  
27 is required in the future to better inform NMVOC/IVOC control policies.

28  
29

### 30 **Acknowledgements**

31 This research has been supported by National Science Foundation of China (21625701 &  
32 21521064), MOST National Key R & D program (2016YFC0207601), Strategic Pilot Project

1 of Chinese Academy of Sciences (XDB05030401), the UCLA Sustainable Los Angeles  
2 Grand Challenge 2016 YZ-50958, and the Jet Propulsion Laboratory, California Institute of  
3 Technology, under contract with NASA. The simulations were completed on the “Explorer  
4 100” cluster system of Tsinghua National Laboratory for Information Science and  
5 Technology.

## 7 **References**

- 8 Burnett, R. T., Pope, C. A., Ezzati, M., Olives, C., Lim, S. S., Mehta, S., Shin, H. H., Singh,  
9 G., Hubbell, B., Brauer, M., Anderson, H. R., Smith, K. R., Balmes, J. R., Bruce, N. G.,  
10 Kan, H. D., Laden, F., Pruss-Ustun, A., Michelle, C. T., Gapstur, S. M., Diver, W. R.,  
11 and Cohen, A.: An Integrated Risk Function for Estimating the Global Burden of  
12 Disease Attributable to Ambient Fine Particulate Matter Exposure, *Environ Health*  
13 *Persp*, 122, 397-403, Doi 10.1289/Ehp.1307049, 2014.
- 14 Cai, S. Y., Wang, Y. J., Zhao, B., Wang, S. X., Chang, X., and Hao, J. M.: The impact of the  
15 "Air Pollution Prevention and Control Action Plan" on PM<sub>2.5</sub> concentrations in Jing-  
16 Jin-Ji region during 2012-2020, *Sci. Total. Environ.*, in press, DOI  
17 10.1016/j.scitotenv.2016.11.188, 2016.
- 18 Cheng, I., Zhang, L., Blanchard, P., Dalziel, J., and Tordon, R.: Concentration-weighted  
19 trajectory approach to identifying potential sources of speciated atmospheric mercury at  
20 an urban coastal site in Nova Scotia, Canada, *Atmos Chem Phys*, 13, 6031-6048,  
21 10.5194/acp-13-6031-2013, 2013.
- 22 Cheng, Y. F., Zheng, G. J., Wei, C., Mu, Q., Zheng, B., Wang, Z. B., Gao, M., Zhang, Q., He,  
23 K. B., Carmichael, G., Pöschl, U., and Su, H.: Reactive nitrogen chemistry in aerosol  
24 water as a source of sulfate during haze events in China, *Sci Adv*, 2, e1601530, DOI:  
25 10.1126/sciadv.1601530, 2016.
- 26 Dong, X. Y., Li, J., Fu, J. S., Gao, Y., Huang, K., and Zhuang, G. S.: Inorganic aerosols  
27 responses to emission changes in Yangtze River Delta, China, *Sci Total Environ*, 481,  
28 522-532, DOI 10.1016/j.scitotenv.2014.02.076, 2014.
- 29 Fu, X., Wang, S. X., Zhao, B., Xing, J., Cheng, Z., Liu, H., and Hao, J. M.: Emission  
30 inventory of primary pollutants and chemical speciation in 2010 for the Yangtze River  
31 Delta region, China, *Atmos Environ*, 70, 39-50, DOI 10.1016/j.atmosenv.2012.12.034,  
32 2013.
- 33 Fu, X., Wang, S. X., Chang, X., Cai, S. Y., Xing, J., and Hao, J. M.: Modeling analysis of  
34 secondary inorganic aerosols over China: pollution characteristics, and meteorological  
35 and dust impacts, *Sci Rep-Uk*, 6, 10.1038/srep35992, 2016.
- 36 Gordon, T. D., Presto, A. A., May, A. A., Nguyen, N. T., Lipsky, E. M., Donahue, N. M.,  
37 Gutierrez, A., Zhang, M., Maddox, C., Rieger, P., Chattopadhyay, S., Maldonado, H.,  
38 Maricq, M. M., and Robinson, A. L.: Secondary organic aerosol formation exceeds  
39 primary particulate matter emissions for light-duty gasoline vehicles, *Atmos Chem Phys*,  
40 14, 4661-4678, DOI 10.5194/acp-14-4661-2014, 2014a.
- 41 Gordon, T. D., Presto, A. A., Nguyen, N. T., Robertson, W. H., Na, K., Sahay, K. N., Zhang,  
42 M., Maddox, C., Rieger, P., Chattopadhyay, S., Maldonado, H., Maricq, M. M., and  
43 Robinson, A. L.: Secondary organic aerosol production from diesel vehicle exhaust:

1 impact of aftertreatment, fuel chemistry and driving cycle, *Atmos Chem Phys*, 14, 4643-  
2 4659, DOI 10.5194/acp-14-4643-2014, 2014b.

3 Guenther, A., Karl, T., Harley, P., Wiedinmyer, C., Palmer, P. I., and Geron, C.: Estimates of  
4 global terrestrial isoprene emissions using MEGAN (Model of Emissions of Gases and  
5 Aerosols from Nature), *Atmos Chem Phys*, 6, 3181-3210, 2006.

6 Hakami, A., Seinfeld, J. H., Chai, T. F., Tang, Y. H., Carmichael, G. R., and Sandu, A.:  
7 Adjoint sensitivity analysis of ozone nonattainment over the continental United States,  
8 *Environ Sci Technol*, 40, 3855-3864, DOI 10.1021/Es052135g, 2006.

9 Han, X., Zhang, M. G., Zhu, L. Y., and Skorokhod, A.: Assessment of the impact of  
10 emissions reductions on air quality over North China Plain, *Atmos Pollut Res*, 7, 249-  
11 259, 10.1016/j.apr.2015.09.009, 2016.

12 Hennigan, C. J., Miracolo, M. A., Engelhart, G. J., May, A. A., Presto, A. A., Lee, T.,  
13 Sullivan, A. P., McMeeking, G. R., Coe, H., Wold, C. E., Hao, W. M., Gilman, J. B.,  
14 Kuster, W. C., de Gouw, J., Schichtel, B. A., Collett, J. L., Kreidenweis, S. M., and  
15 Robinson, A. L.: Chemical and physical transformations of organic aerosol from the  
16 photo-oxidation of open biomass burning emissions in an environmental chamber,  
17 *Atmos Chem Phys*, 11, 7669-7686, DOI 10.5194/acp-11-7669-2011, 2011.

18 Iman, R. L., Davenport, J. M., and Zeigler, D. K.: Latin Hypercube Sampling (Program User's  
19 Guide), Sandia National Laboratories, Albuquerque, NM, U.S., 78 pp., 1980.

20 IPCC: Climate Change 2013: The Physical Science Basis. Contribution of Working Group I  
21 to the Fifth Assessment Report of the Intergovernmental Panel on Climate Change,  
22 edited by: Stocker, T. F., Qin, D., Plattner, G.-K., Tignor, M., Allen, S. K., Boschung, J.,  
23 Nauels, A., Xia, Y., Bex, V., and Midgley, P. M., Cambridge University Press,  
24 Cambridge, United Kingdom and New York, NY, USA, 1535 pp., 2013.

25 Jathar, S. H., Gordon, T. D., Hennigan, C. J., Pye, H. O. T., Pouliot, G., Adams, P. J.,  
26 Donahue, N. M., and Robinson, A. L.: Unspeciated organic emissions from combustion  
27 sources and their influence on the secondary organic aerosol budget in the United States,  
28 *P Natl Acad Sci USA*, 111, 10473-10478, DOI 10.1073/pnas.1323740111, 2014.

29 Jia, Y. T., Rahn, K. A., He, K. B., Wen, T. X., and Wang, Y. S.: A novel technique for  
30 quantifying the regional component of urban aerosol solely from its sawtooth cycles, *J*  
31 *Geophys Res-Atmos*, 113, 10.1029/2008jd010389, 2008.

32 Li, J. W., and Han, Z. W.: A modeling study of severe winter haze events in Beijing and its  
33 neighboring regions, *Atmos Res*, 170, 87-97, 10.1016/j.atmosres.2015.11.009, 2016.

34 Li, M., Zhang, Q., Kurokawa, J., Woo, J. H., He, K. B., Lu, Z., Ohara, T., Song, Y., Streets, D.  
35 G., Carmichael, G. R., Cheng, Y. F., Hong, C. P., Huo, H., Jiang, X. J., Kang, S. C., Liu,  
36 F., Su, H., and Zheng, B.: MIX: a mosaic Asian anthropogenic emission inventory for  
37 the MICS-Asia and the HTAP projects, *Atmos Chem Phys Discuss*, 15, 34813-34869,  
38 doi:10.5194/acpd-15-34813-2015, 2015a.

39 Li, X., Zhang, Q., Zhang, Y., Zheng, B., Wang, K., Chen, Y., Wallington, T. J., Han, W. J.,  
40 Shen, W., Zhang, X. Y., and He, K. B.: Source contributions of urban PM<sub>2.5</sub> in the  
41 Beijing-Tianjin-Hebei region: Changes between 2006 and 2013 and relative impacts of  
42 emissions and meteorology, *Atmos Environ*, 123, 229-239,  
43 10.1016/j.atmosenv.2015.10.048, 2015b.

44 Lim, S. S., Vos, T., Flaxman, A. D., Danaei, G., Shibuya, K., Adair-Rohani, H., AlMazroa, M.  
45 A., Amann, M., Anderson, H. R., Andrews, K. G., Aryee, M., Atkinson, C., Bacchus, L.  
46 J., Bahalim, A. N., Balakrishnan, K., Balmes, J., Barker-Collo, S., Baxter, A., Bell, M.  
47 L., Blore, J. D., Blyth, F., Bonner, C., Borges, G., Bourne, R., Boussinesq, M., Brauer,  
48 M., Brooks, P., Bruce, N. G., Brunekreef, B., Bryan-Hancock, C., Bucello, C.,

1 Buchbinder, R., Bull, F., Burnett, R. T., Byers, T. E., Calabria, B., Carapetis, J.,  
2 Carnahan, E., Chafe, Z., Charlson, F., Chen, H., Chen, J. S., Cheng, A. T.-A., Child, J.  
3 C., Cohen, A., Colson, K. E., Cowie, B. C., Darby, S., Darling, S., Davis, A.,  
4 Degenhardt, L., Dentener, F., Des Jarlais, D. C., Devries, K., Dherani, M., Ding, E. L.,  
5 Dorsey, E. R., Driscoll, T., Edmond, K., Ali, S. E., Engell, R. E., Erwin, P. J., Fahimi, S.,  
6 Falder, G., Farzadfar, F., Ferrari, A., Finucane, M. M., Flaxman, S., Fowkes, F. G. R.,  
7 Freedman, G., Freeman, M. K., Gakidou, E., Ghosh, S., Giovannucci, E., Gmel, G.,  
8 Graham, K., Grainger, R., Grant, B., Gunnell, D., Gutierrez, H. R., Hall, W., Hoek, H.  
9 W., Hogan, A., Hosgood Iii, H. D., Hoy, D., Hu, H., Hubbell, B. J., Hutchings, S. J.,  
10 Ibeanusi, S. E., Jacklyn, G. L., Jasrasaria, R., Jonas, J. B., Kan, H., Kanis, J. A.,  
11 Kassebaum, N., Kawakami, N., Khang, Y.-H., Khatibzadeh, S., Khoo, J.-P., Kok, C.,  
12 Laden, F., Lalloo, R., Lan, Q., Lathlean, T., Leasher, J. L., Leigh, J., Li, Y., Lin, J. K.,  
13 Lipshultz, S. E., London, S., Lozano, R., Lu, Y., Mak, J., Malekzadeh, R., Mallinger, L.,  
14 Marcenes, W., March, L., Marks, R., Martin, R., McGale, P., McGrath, J., Mehta, S.,  
15 Memish, Z. A., Mensah, G. A., Merriman, T. R., Micha, R., Michaud, C., Mishra, V.,  
16 Hanafiah, K. M., Mokdad, A. A., Morawska, L., Mozaffarian, D., Murphy, T., Naghavi,  
17 M., Neal, B., Nelson, P. K., Nolla, J. M., Norman, R., Olives, C., Omer, S. B., Orchard,  
18 J., Osborne, R., Ostro, B., Page, A., Pandey, K. D., Parry, C. D. H., Passmore, E., Patra,  
19 J., Pearce, N., Pelizzari, P. M., Petzold, M., Phillips, M. R., Pope, D., Pope Iii, C. A.,  
20 Powles, J., Rao, M., Razavi, H., Rehfuss, E. A., Rehm, J. T., Ritz, B., Rivara, F. P.,  
21 Roberts, T., Robinson, C., Rodriguez-Portales, J. A., Romieu, I., Room, R., Rosenfeld,  
22 L. C., Roy, A., Rushton, L., Salomon, J. A., Sampson, U., Sanchez-Riera, L., Sanman,  
23 E., Sapkota, A., Seedat, S., Shi, P., Shield, K., Shivakoti, R., Singh, G. M., Sleet, D. A.,  
24 Smith, E., Smith, K. R., Stapelberg, N. J. C., Steenland, K., Stöckl, H., Stovner, L. J.,  
25 Straif, K., Straney, L., Thurston, G. D., Tran, J. H., Van Dingenen, R., van Donkelaar,  
26 A., Veerman, J. L., Vijayakumar, L., Weintraub, R., Weissman, M. M., White, R. A.,  
27 Whiteford, H., Wiersma, S. T., Wilkinson, J. D., Williams, H. C., Williams, W., Wilson,  
28 N., Woolf, A. D., Yip, P., Zielinski, J. M., Lopez, A. D., Murray, C. J. L., and Ezzati,  
29 M.: A comparative risk assessment of burden of disease and injury attributable to 67 risk  
30 factors and risk factor clusters in 21 regions, 1990–2010: a systematic analysis for the  
31 Global Burden of Disease Study 2010, *The Lancet*, 380, 2224-2260,  
32 [http://dx.doi.org/10.1016/S0140-6736\(12\)61766-8](http://dx.doi.org/10.1016/S0140-6736(12)61766-8), 2012.

33 Liu, J., Mauzerall, D. L., Chen, Q., Zhang, Q., Song, Y., Peng, W., Klimont, Z., Qiu, X. H.,  
34 Zhang, S. Q., Hu, M., Lin, W. L., Smith, K. R., and Zhu, T.: Air pollutant emissions  
35 from Chinese households: A major and underappreciated ambient pollution source, *P*  
36 *Natl Acad Sci USA*, 113, 7756-7761, 10.1073/pnas.1604537113, 2016.

37 Lv, L. Y., and Li, H. Y.: Economic evaluation of the health effect of PM10 and PM2.5  
38 pollution over the Beijing-Tianjin-Hebei region, *Acta Scientiarum Naturalium*  
39 *Universitatis Nankaiensis*, 69-77, 2016.

40 Qin, Y., and Xie, S. D.: Historical estimation of carbonaceous aerosol emissions from  
41 biomass open burning in China for the period 1990-2005, *Environ Pollut*, 159, 3316-  
42 3323, DOI 10.1016/j.envpol.2011.08.042, 2011.

43 Russell, A., Milford, J., Bergin, M. S., Mcbride, S., Mcnair, L., Yang, Y., Stockwell, W. R.,  
44 and Croes, B.: Urban Ozone Control and Atmospheric Reactivity of Organic Gases,  
45 *Science*, 269, 491-495, DOI 10.1126/science.269.5223.491, 1995.

46 Sandu, A., Daescu, D. N., Carmichael, G. R., and Chai, T. F.: Adjoint sensitivity analysis of  
47 regional air quality models, *J Comput Phys*, 204, 222-252, DOI  
48 10.1016/j.jcp.2004.10.011, 2005.

- 1 Santner, T. J., Williams, B. J., and Notz, W.: The Design and Analysis of Computer  
2 Experiments, Springer Verlag, New York, U.S., 283 pp., 2003.
- 3 Stein, A. F., Draxler, R. R., Rolph, G. D., Stunder, B. J. B., Cohen, M. D., and Ngan, F.:  
4 NOAA's HYSPLIT atmospheric transport and dispersion modeling system, B Am  
5 Meteorol Soc, 96, 2059-2077, 10.1175/bams-d-14-00110.1, 2015.
- 6 Streets, D. G., Fu, J. S., Jang, C. J., Hao, J. M., He, K. B., Tang, X. Y., Zhang, Y. H., Wang,  
7 Z. F., Li, Z. P., and Zhang, Q.: Air quality during the 2008 Beijing Olympic Games,  
8 Atmos Environ, 41, 480-492, DOI 10.1016/j.atmosenv.2006.08.046, 2007.
- 9 The State Council of the People's Republic of China: Notice to issue the "Air Pollution  
10 Prevention and Control Action Plan": [http://www.gov.cn/zwggk/2013-  
11 09/12/content\\_2486773.htm](http://www.gov.cn/zwggk/2013-09/12/content_2486773.htm), access: September 9, 2016, 2013.
- 12 U.S. Environmental Protection Agency: Technical support document for the proposed PM  
13 NAAQS rule: Response Surface Modeling[R/OL]:  
14 [http://www.epa.gov/scram001/reports/pmnaqs\\_tsd\\_rsm\\_all\\_021606.pdf](http://www.epa.gov/scram001/reports/pmnaqs_tsd_rsm_all_021606.pdf), access: 2015-  
15 02-01, 2006.
- 16 van Donkelaar, A., Martin, R. V., Brauer, M., and Boys, B. L.: Use of satellite observations  
17 for long-term exposure assessment of global concentrations of fine particulate matter,  
18 Environmental health perspectives, 123, 135, 2015.
- 19 Wang, G. H., Zhang, R. Y., Gomez, M. E., Yang, L. X., Zamora, M. L., Hu, M., Lin, Y., Peng,  
20 J. F., Guo, S., Meng, J. J., Li, J. J., Cheng, C. L., Hu, T. F., Ren, Y. Q., Wang, Y. S.,  
21 Gao, J., Cao, J. J., An, Z. S., Zhou, W. J., Li, G. H., Wang, J. Y., Tian, P. F., Marrero-  
22 Ortiz, W., Secrest, J., Du, Z. F., Zheng, J., Shang, D. J., Zeng, L. M., Shao, M., Wang,  
23 W. G., Huang, Y., Wang, Y., Zhu, Y. J., Li, Y. X., Hu, J. X., Pan, B., Cai, L., Cheng, Y.  
24 T., Ji, Y. M., Zhang, F., Rosenfeld, D., Liss, P. S., Duce, R. A., Kolb, C. E., and Molina,  
25 M. J.: Persistent sulfate formation from London Fog to Chinese haze, P Natl Acad Sci  
26 USA, 113, 13630-13635, 10.1073/pnas.1616540113, 2016a.
- 27 Wang, J. D., Xing, J., Mathur, R., Pleim, J. E., Wang, S. X., Hogrefe, C., Gan, C.-M., Wong,  
28 D. C., and Hao, J. M.: Historical Trends in PM<sub>2.5</sub>-Related Premature Mortality during  
29 1990-2010 across the Northern Hemisphere, Environ Health Persp, in press, DOI  
30 10.1289/EHP298, 2016b.
- 31 Wang, J. D., Zhao, B., Wang, S. X., Yang, F. M., Xing, J., Morawska, L., Ding, A. J.,  
32 Kulmala, M., Kerminen, V. M., Kujansuu, J., Wang, Z. F., Ding, D. A., Zhang, X. Y.,  
33 Wang, H. B., Tian, M., Petaja, T., Jiang, J. K., and Hao, J. M.: Particulate matter  
34 pollution over China and the effects of control policies, Sci Total Environ, 584, 426-447,  
35 10.1016/j.scitotenv.2017.01.027, 2017a.
- 36 Wang, J. D., Zhao, B., Yang, F. M., Xing, J., Morawska, L., Ding, A. J., Kulmala, M.,  
37 Kerminen, V.-M., Kujansuu, J., Wang, Z. F., Ding, D., Zhang, X. Y., Wang, H. B., Tian,  
38 M., Petäjä, T., Jiang, J. K., and Hao, J. M.: Particulate matter pollution over China and  
39 the effects of control policies, Sci Total Environ, in press, DOI  
40 10.1016/j.scitotenv.2017.01.027, 2017b.
- 41 Wang, L. T., Hao, J. M., He, K. B., Wang, S. X., Li, J. H., Zhang, Q., Streets, D. G., Fu, J. S.,  
42 Jang, C. J., Takekawa, H., and Chatani, S.: A modeling study of coarse particulate  
43 matter pollution in Beijing: Regional source contributions and control implications for  
44 the 2008 summer Olympics, J Air Waste Manage, 58, 1057-1069, Doi 10.3155/1047-  
45 3289.58.8.1057, 2008.
- 46 Wang, L. T., Jang, C., Zhang, Y., Wang, K., Zhang, Q. A., Streets, D., Fu, J., Lei, Y.,  
47 Schreifels, J., He, K. B., Hao, J. M., Lam, Y. F., Lin, J., Meskhidze, N., Voorhees, S.,  
48 Evarts, D., and Phillips, S.: Assessment of air quality benefits from national air pollution

1 control policies in China. Part II: Evaluation of air quality predictions and air quality  
2 benefits assessment, *Atmos Environ*, 44, 3449-3457, DOI  
3 10.1016/j.atmosenv.2010.05.058, 2010.

4 Wang, L. T., Wei, Z., Yang, J., Zhang, Y., Zhang, F. F., Su, J., Meng, C. C., and Zhang, Q.:  
5 The 2013 severe haze over southern Hebei, China: model evaluation, source  
6 apportionment, and policy implications, *Atmos Chem Phys*, 14, 3151-3173,  
7 10.5194/acp-14-3151-2014, 2014a.

8 Wang, S. X., and Zhang, C. Y.: Spatial and temporal distribution of air pollutant emissions  
9 from open burning of crop residues in China, *Sciencepaper Online*, 3, 1-6, 2008.

10 Wang, S. X., Xing, J., Jang, C. R., Zhu, Y., Fu, J. S., and Hao, J. M.: Impact assessment of  
11 ammonia emissions on inorganic aerosols in east China using response surface modeling  
12 technique, *Environ Sci Technol*, 45, 9293-9300, DOI 10.1021/Es2022347, 2011.

13 Wang, S. X., Zhao, B., Cai, S. Y., Klimont, Z., Nielsen, C. P., Morikawa, T., Woo, J. H., Kim,  
14 Y., Fu, X., Xu, J. Y., Hao, J. M., and He, K. B.: Emission trends and mitigation options  
15 for air pollutants in East Asia, *Atmos Chem Phys*, 14, 6571-6603, DOI 10.5194/acp-14-  
16 6571-2014, 2014b.

17 Wang, Y. J., Bao, S. W., Wang, S. X., Hu, Y. T., Shi, X., Wang, J. D., Zhao, B., Jiang, J. K.,  
18 Zheng, M., Wu, M. H., Russell, A. G., Wang, Y. H., and Hao, J. M.: Local and regional  
19 contributions to fine particulate matter in Beijing during heavy haze episodes, *Sci Total*  
20 *Environ*, in press, DOI: 10.1016/j.scitotenv.2016.12.127, 2016c.

21 Wu, W. J.: Health Effect Attributed to Ambient Fine Particle Pollution in the Beijing-Tianjin-  
22 Hebei Region and its Source Apportionment, Doctor, School of Environment, Tsinghua  
23 University, Beijing, China, 98 pp., 2016.

24 Xing, J., Wang, S. X., Jang, C., Zhu, Y., and Hao, J. M.: Nonlinear response of ozone to  
25 precursor emission changes in China: a modeling study using response surface  
26 methodology, *Atmos Chem Phys*, 11, 5027-5044, DOI 10.5194/acp-11-5027-2011,  
27 2011.

28 Yang, Y. J., Wilkinson, J. G., and Russell, A. G.: Fast, direct sensitivity analysis of  
29 multidimensional photochemical models, *Environ Sci Technol*, 31, 2859-2868, DOI  
30 10.1021/Es970117w, 1997.

31 Ying, Q., Wu, L., and Zhang, H. L.: Local and inter-regional contributions to PM<sub>2.5</sub> nitrate  
32 and sulfate in China, *Atmos Environ*, 94, 582-592, 10.1016/j.atmosenv.2014.05.078,  
33 2014.

34 Yu, L. D., Wang, G. F., Zhang, R. J., Zhang, L. M., Song, Y., Wu, B. B., Li, X. F., An, K.,  
35 and Chu, J. H.: Characterization and Source Apportionment of PM<sub>2.5</sub> in an Urban  
36 Environment in Beijing, *Aerosol Air Qual Res*, 13, 574-583, 10.4209/aaqr.2012.07.0192,  
37 2013.

38 Zhang, L., Shao, J. Y., Lu, X., Zhao, Y. H., Hu, Y. Y., Henze, D. K., Liao, H., Gong, S. L.,  
39 and Zhang, Q.: Sources and Processes Affecting Fine Particulate Matter Pollution over  
40 North China: An Adjoint Analysis of the Beijing APEC Period, *Environ Sci Technol*, 50,  
41 8731-8740, 10.1021/acs.est.6b03010, 2016.

42 Zhang, W., Guo, J. H., Sun, Y. L., Yuan, H., Zhuang, G. S., Zhuang, Y. H., and Hao, Z. P.:  
43 Source apportionment for urban PM<sub>10</sub> and PM<sub>2.5</sub> in the Beijing area, *Chinese Sci Bull*,  
44 52, 608-615, 10.1007/s11434-007-0076-5, 2007.

45 Zhao, B., Wang, S. X., Dong, X. Y., Wang, J. D., Duan, L., Fu, X., Hao, J. M., and Fu, J.:  
46 Environmental effects of the recent emission changes in China: implications for  
47 particulate matter pollution and soil acidification, *Environ Res Lett*, 8, 024031, DOI  
48 10.1088/1748-9326/8/2/024031, 2013a.

1 Zhao, B., Wang, S. X., Liu, H., Xu, J. Y., Fu, K., Klimont, Z., Hao, J. M., He, K. B., Cofala,  
2 J., and Amann, M.: NO<sub>x</sub> emissions in China: historical trends and future perspectives,  
3 *Atmos Chem Phys*, 13, 9869-9897, DOI 10.5194/acp-13-9869-2013, 2013b.

4 Zhao, B., Wang, S. X., Wang, J. D., Fu, J. S., Liu, T. H., Xu, J. Y., Fu, X., and Hao, J. M.:  
5 Impact of national NO<sub>x</sub> and SO<sub>2</sub> control policies on particulate matter pollution in  
6 China, *Atmos Environ*, 77, 453-463, DOI 10.1016/j.atmosenv.2013.05.012, 2013c.

7 Zhao, B., Wang, S. X., Donahue, N. M., Chuang, W., Hildebrandt Ruiz, L., Ng, N. L., Wang,  
8 Y. J., and Hao, J. M.: Evaluation of one-dimensional and two-dimensional volatility  
9 basis sets in simulating the aging of secondary organic aerosols with smog-chamber  
10 experiments, *Environ Sci Technol*, 49, 2245-2254, DOI 10.1021/es5048914, 2015a.

11 Zhao, B., Wang, S. X., Xing, J., Fu, K., Fu, J. S., Jang, C., Zhu, Y., Dong, X. Y., Gao, Y., Wu,  
12 W. J., Wang, J. D., and Hao, J. M.: Assessing the nonlinear response of fine particles to  
13 precursor emissions: development and application of an extended response surface  
14 modeling technique v1.0, *Geosci Model Dev*, 8, 115-128, DOI 10.5194/gmd-8-115-  
15 2015, 2015b.

16 Zhao, B., Wang, S. X., Donahue, N. M., Jathar, S. H., Huang, X. F., Wu, W. J., Hao, J. M.,  
17 and Robinson, A. L.: Quantifying the effect of organic aerosol aging and intermediate-  
18 volatility emissions on regional-scale aerosol pollution in China, *Sci Rep-Uk*, 6,  
19 10.1038/srep28815, 2016.

20 Zhao, Y., Wang, S. X., Duan, L., Lei, Y., Cao, P. F., and Hao, J. M.: Primary air pollutant  
21 emissions of coal-fired power plants in China: Current status and future prediction,  
22 *Atmos Environ*, 42, 8442-8452, DOI 10.1016/j.atmosenv.2008.08.021, 2008.

23 Zheng, G. J., Duan, F. K., Su, H., Ma, Y. L., Cheng, Y., Zheng, B., Zhang, Q., Huang, T.,  
24 Kimoto, T., Chang, D., Poschl, U., Cheng, Y. F., and He, K. B.: Exploring the severe  
25 winter haze in Beijing: the impact of synoptic weather, regional transport and  
26 heterogeneous reactions, *Atmos Chem Phys*, 15, 2969-2983, 10.5194/acp-15-2969-2015,  
27 2015.

28  
29  
30



1 **Tables and figures**

2 Table 1. Description of the RSM/ERSM prediction systems developed in this study.

Method	Control variables	Control scenarios
Conventional RSM technique	5 control variables: total emissions of NO <sub>x</sub> , SO <sub>2</sub> , NH <sub>3</sub> , NMVOC+IVOC, and POA	101 control scenarios: 1) 1 CMAQ/2D-VBS base case; 2) 100 <sup>a</sup> scenarios generated by applying LHS method for the 5 variables.
ERSM technique	55 control variables in total: 11 control variables in each of the 5 regions, including 7 nonlinear control variables, i.e., 1) NO <sub>x</sub> /large point sources (LPS) <sup>b</sup> 2) NO <sub>x</sub> /other sources 3) SO <sub>2</sub> /LPS 4) SO <sub>2</sub> /other sources 5) NH <sub>3</sub> /all sources 6) NMVOC+IVOC/all sources 7) POA/all sources and 4 linear control variables, i.e., 8) Primary inorganic PM <sub>2.5</sub> /power plants 9) Primary inorganic PM <sub>2.5</sub> /Industry 10) Primary inorganic PM <sub>2.5</sub> /residential & commercial 11) Primary inorganic PM <sub>2.5</sub> /transportation	1121 control scenarios: 1) 1 CMAQ/2D-VBS base case; 2) 1000 scenarios, including 200 <sup>a</sup> scenarios generated by applying LHS method for the nonlinear control variables in Beijing, 200 scenarios generated in the same way for Tianjin, 200 scenarios for Northern Hebei, 200 scenarios for Southern Hebei, and 200 scenarios for Eastern Hebei; 3) 100 <sup>a</sup> scenarios generated by applying LHS method for the total emissions of NO <sub>x</sub> , SO <sub>2</sub> , NH <sub>3</sub> , NMVOC+IVOC, and POA; 4) 20 scenarios where one primary inorganic PM <sub>2.5</sub> control variable is set to 0.25 for each scenario.

3 <sup>a</sup> 100 and 200 scenarios are needed for the response surfaces for 5 and 7 variables, respectively (Xing et al.,  
4 2011; Wang et al., 2011).

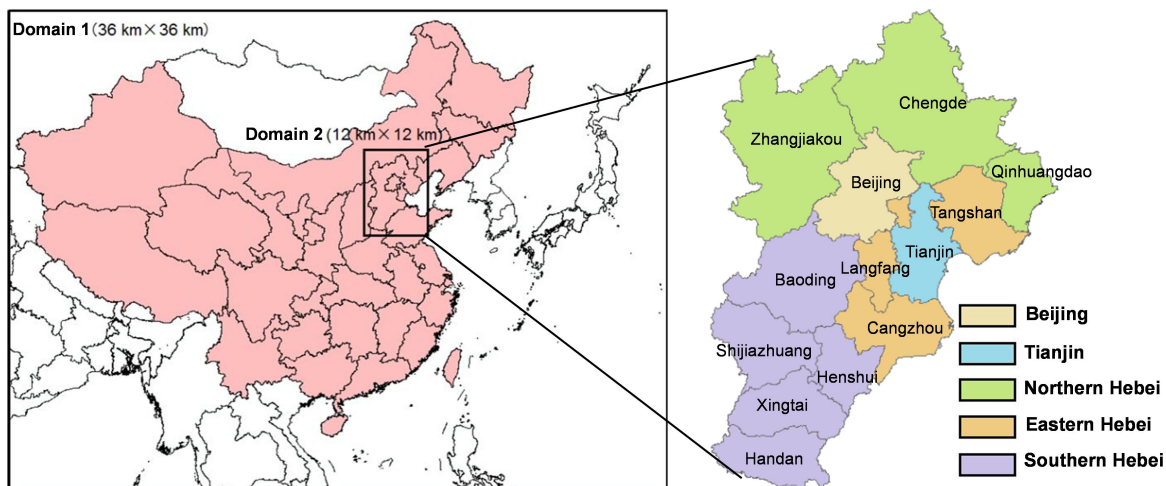
5 <sup>b</sup> LPS includes power plants, iron and steel plants, and cement plants

6

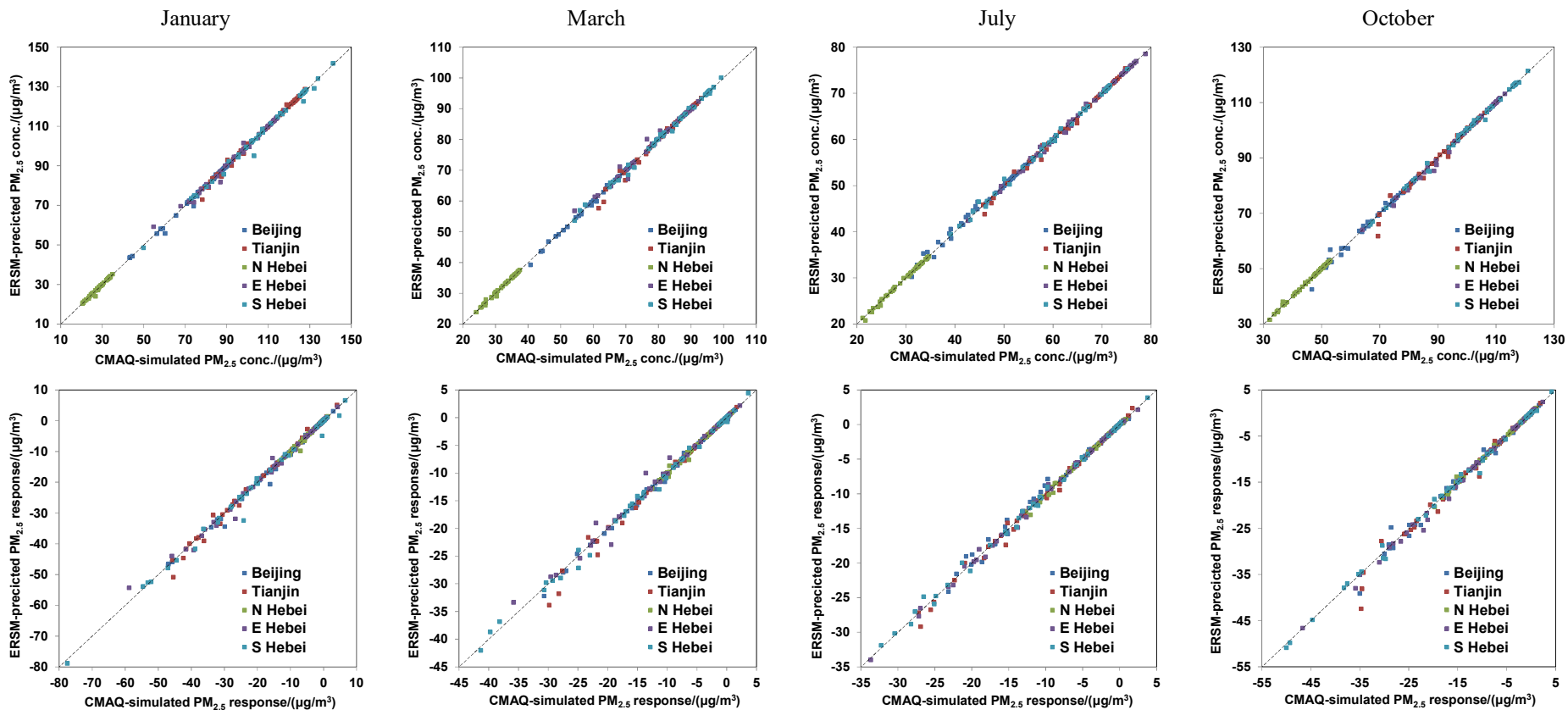
1 Table 2. Comparison between ERSM-predicted and CMAQ/2D-VBS-simulated PM<sub>2.5</sub> concentrations for  
 2 54 out-of-sample scenarios.

Month	Variable	Statistical index	Beijing	Tianjin	Northern Hebei	Eastern Hebei	Southern Hebei	
Jan	PM <sub>2.5</sub> concentration	R	0.998	0.998	0.995	0.997	0.997	
		MNE (%)	0.52	0.55	0.64	0.67	0.60	
		Maximum NE (%)	7.56	6.98	10.67	8.01	8.03	
		95% percentile of NEs (%)	1.61	2.86	2.92	3.46	3.02	
		NME (%)	0.44	0.46	0.57	0.53	0.53	
	PM <sub>2.5</sub> response	R	0.998	0.998	0.995	0.997	0.997	
		NME (%)	3.36	3.48	4.25	4.00	3.88	
	Mar	PM <sub>2.5</sub> concentration	R	0.999	0.996	0.998	0.995	0.999
			MNE (%)	0.37	0.54	0.39	0.57	0.49
			Maximum NE (%)	3.75	6.58	4.30	5.04	3.22
95% percentile of NEs (%)			1.53	3.15	2.03	4.35	2.03	
NME (%)			0.31	0.45	0.34	0.49	0.42	
PM <sub>2.5</sub> response		R	0.999	0.996	0.998	0.995	0.999	
		NME (%)	2.38	4.32	2.70	4.55	3.59	
Jul		PM <sub>2.5</sub> concentration	R	0.997	0.998	0.998	0.999	0.999
			MNE (%)	0.94	0.54	0.46	0.37	0.47
			Maximum NE (%)	5.05	5.02	4.65	1.83	3.62
	95% percentile of NEs (%)		3.47	2.33	2.17	1.49	1.87	
	NME (%)		0.80	0.47	0.41	0.33	0.39	
	PM <sub>2.5</sub> response	R	0.997	0.998	0.998	0.999	0.999	
		NME (%)	4.97	3.71	2.80	2.58	2.78	
	Oct	PM <sub>2.5</sub> concentration	R	0.996	0.994	0.999	0.999	0.999
			MNE (%)	0.83	0.70	0.36	0.39	0.36
			Maximum NE (%)	8.90	11.19	3.79	3.90	2.46
95% percentile of NEs (%)			3.04	3.50	1.44	2.10	1.64	
NME (%)			0.67	0.58	0.30	0.35	0.32	
PM <sub>2.5</sub> response		R	0.996	0.994	0.999	0.999	0.999	
		NME (%)	4.51	5.64	2.20	3.29	2.79	

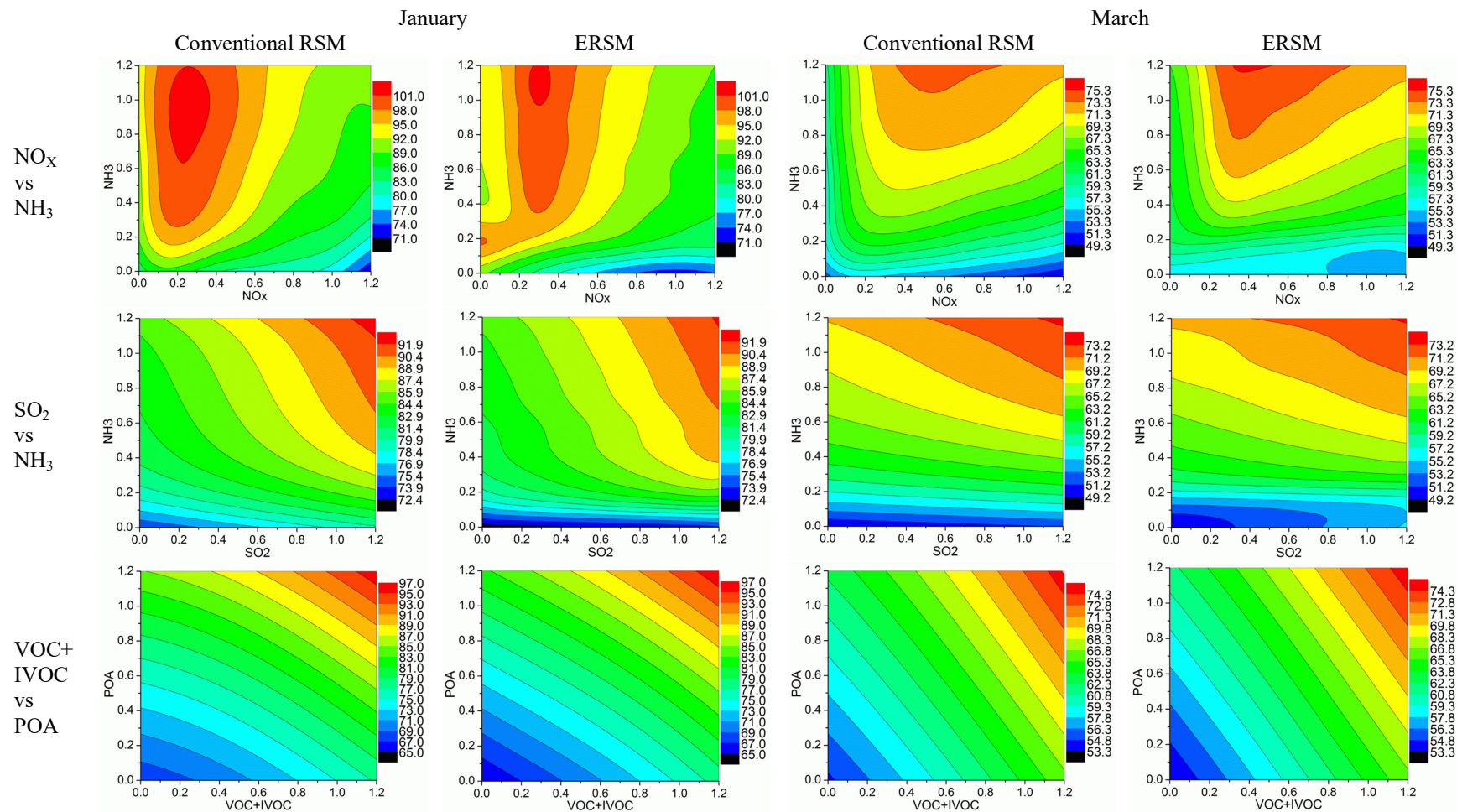
3



1  
 2 Figure 1. Double nesting domains used in CMAQ/2D-VBS simulation (left) and the definition  
 3 of five target regions in the innermost domain, denoted by different colours (right). The grey  
 4 lines in the right figure represent the boundaries of prefecture-level cities.

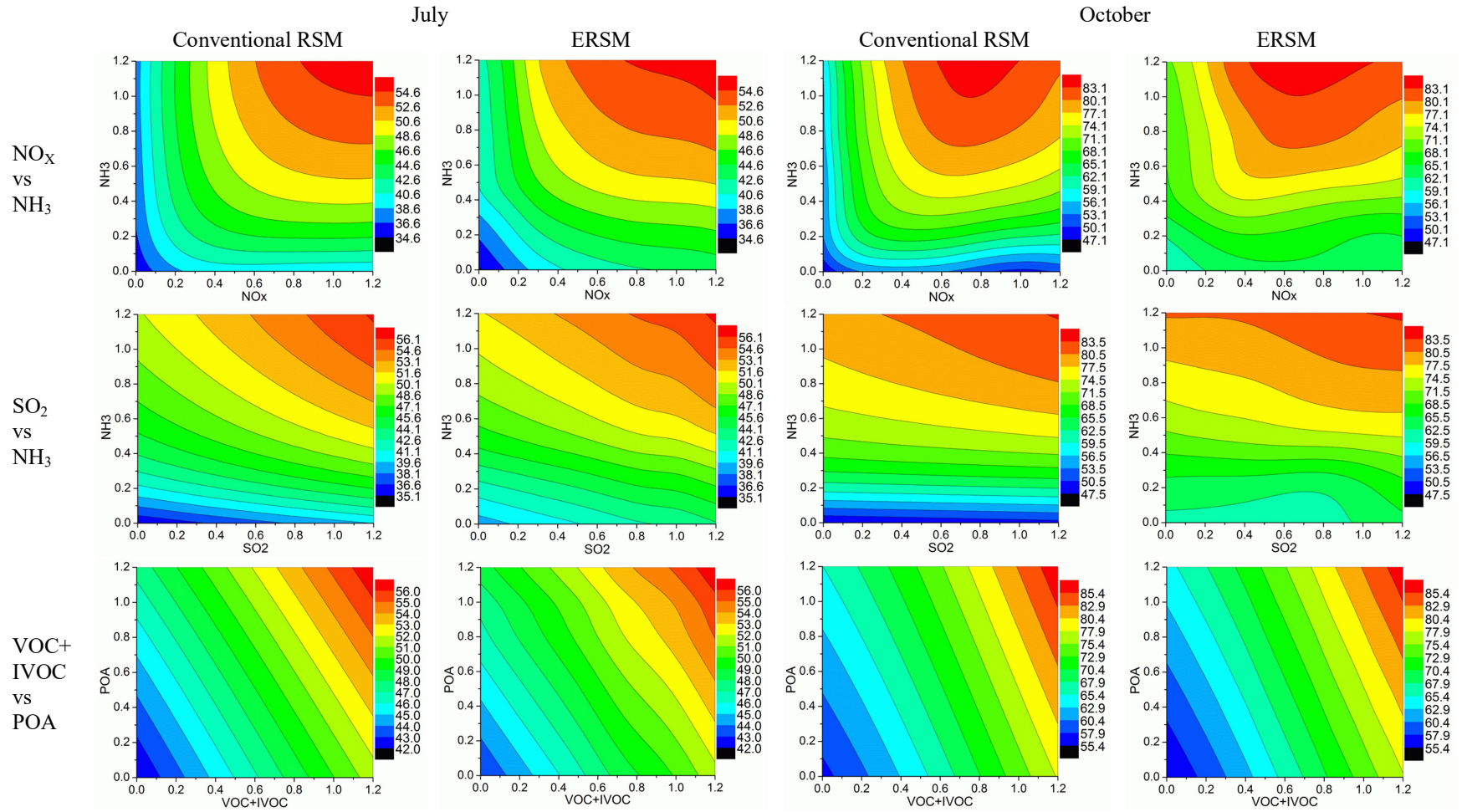


1 Figure 2. Comparison of  $PM_{2.5}$  concentrations (top row) and  $PM_{2.5}$  responses (bottom row) predicted by the ERSM technique with out-of-  
 2 sample CMAQ/2D-VBS simulations. The dashed line is the one-to-one line indicating perfect agreement.

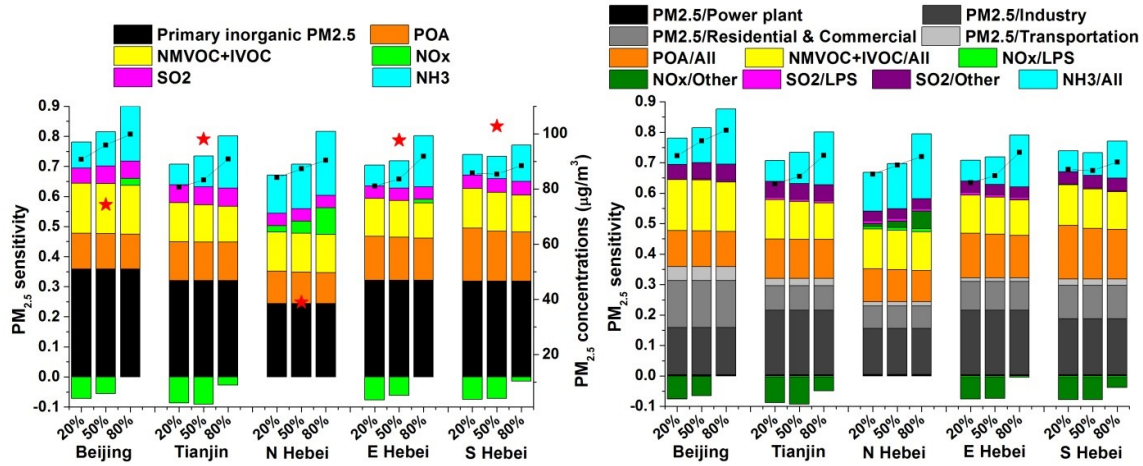


1 Figure 3. Comparison of the 2-D isopleths of  $PM_{2.5}$  concentrations in Beijing in response to the simultaneous changes of precursor  
 2 emissions in all five regions derived from the conventional RSM technique and the ERSM technique. The X- and Y-axis represent the  
 3 emission ratio, defined as the ratios of the changed emissions to the emissions in the base case. The colour contours represent  $PM_{2.5}$   
 4 concentrations (unit:  $\mu g m^{-3}$ ).

1



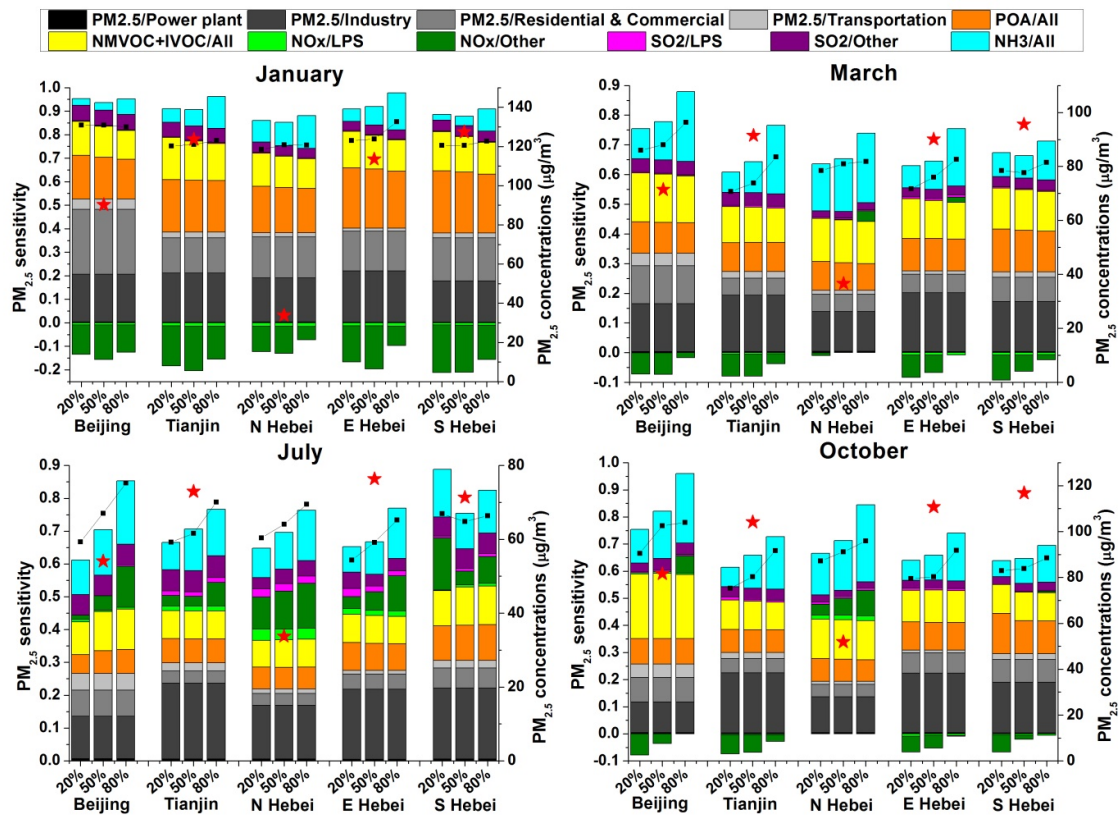
2 Figure 3. Continued.



1  
 2 Figure 4. Sensitivity of 4-month mean  $PM_{2.5}$  concentrations to stepped control of individual  
 3 air pollutants (left) and individual pollutant-sector combinations (right). The X-axis shows the  
 4 reduction ratio ( $= 1 - \text{emission ratio}$ ). The Y-axis shows  $PM_{2.5}$  sensitivity, which is defined as  
 5 the change ratio of concentration divided by the reduction ratio of emissions. The coloured  
 6 bars denote the  $PM_{2.5}$  sensitivities when a particular emission source is controlled while the  
 7 others stay the same as the base case; the black dotted line denotes the  $PM_{2.5}$  sensitivity when  
 8 all emission sources are controlled simultaneously. The red stars represent  $PM_{2.5}$   
 9 concentrations in the base case.

10

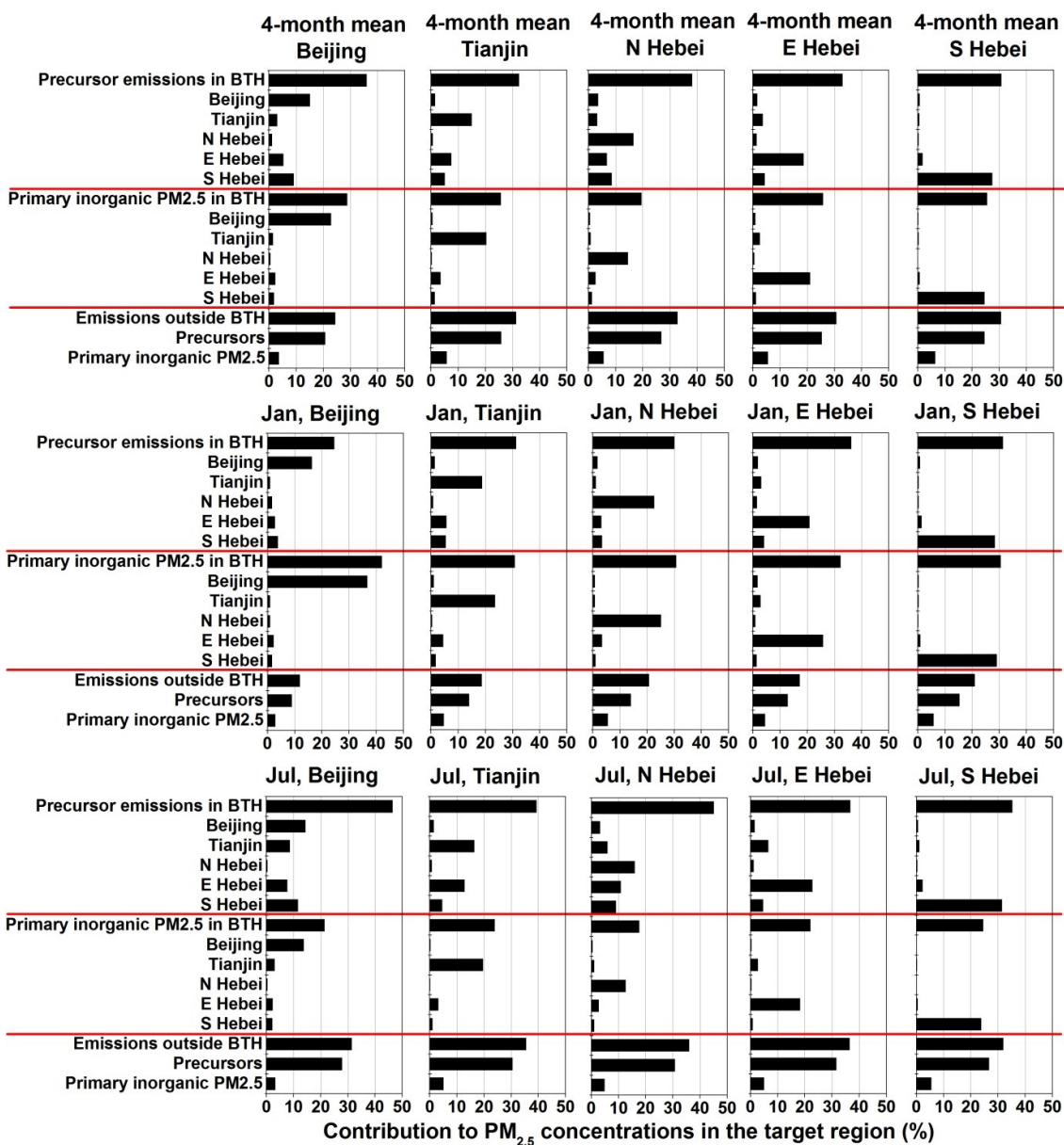




1  
 2 Figure 5. Sensitivity of monthly mean  $PM_{2.5}$  concentrations to stepped control of individual  
 3 air pollutants from individual sectors in January, March, July, and October. The meanings of  
 4 X-axis, Y-axis, coloured bars, black dotted lines, and red stars are the same as Fig. 4.

5

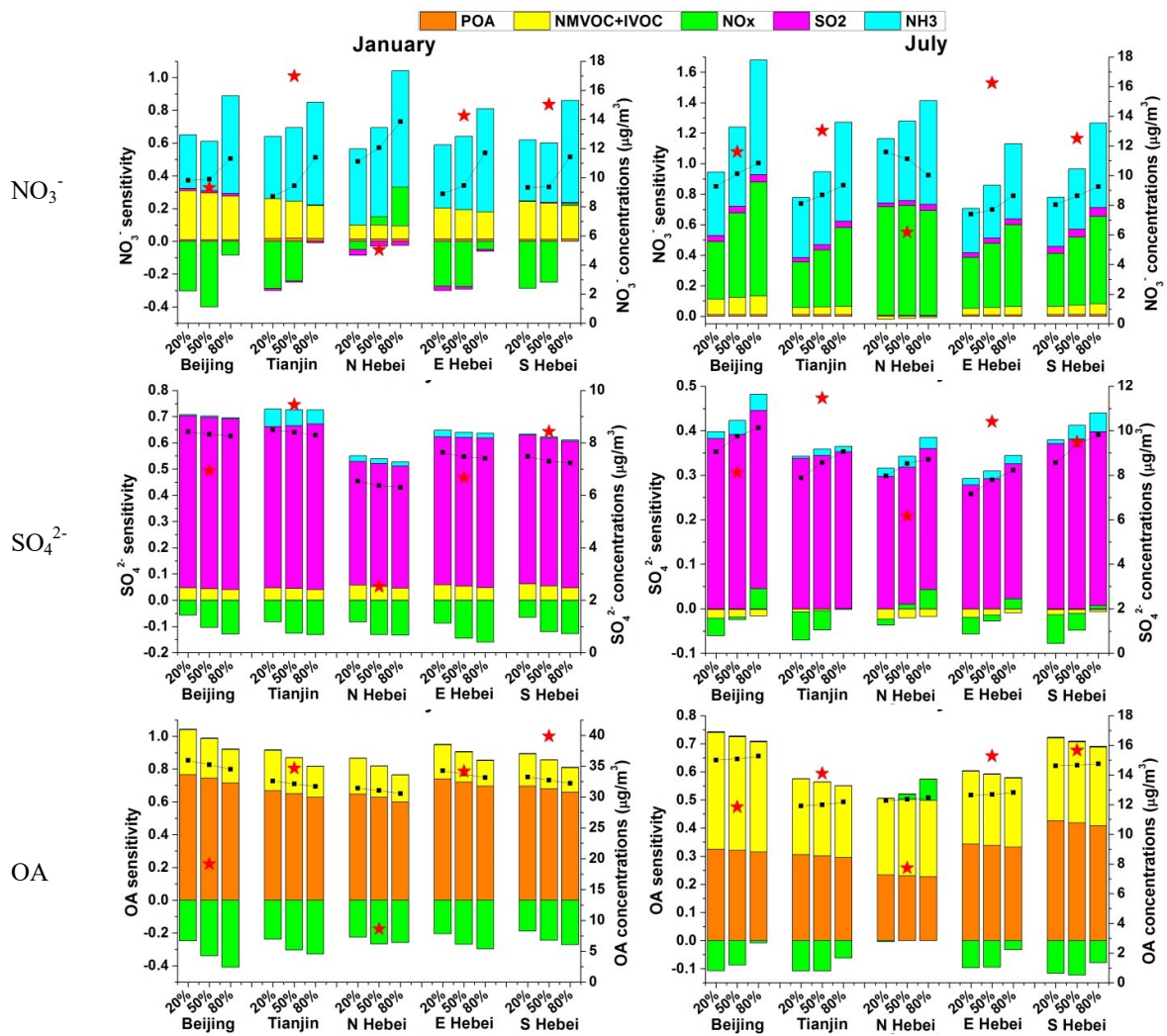




1

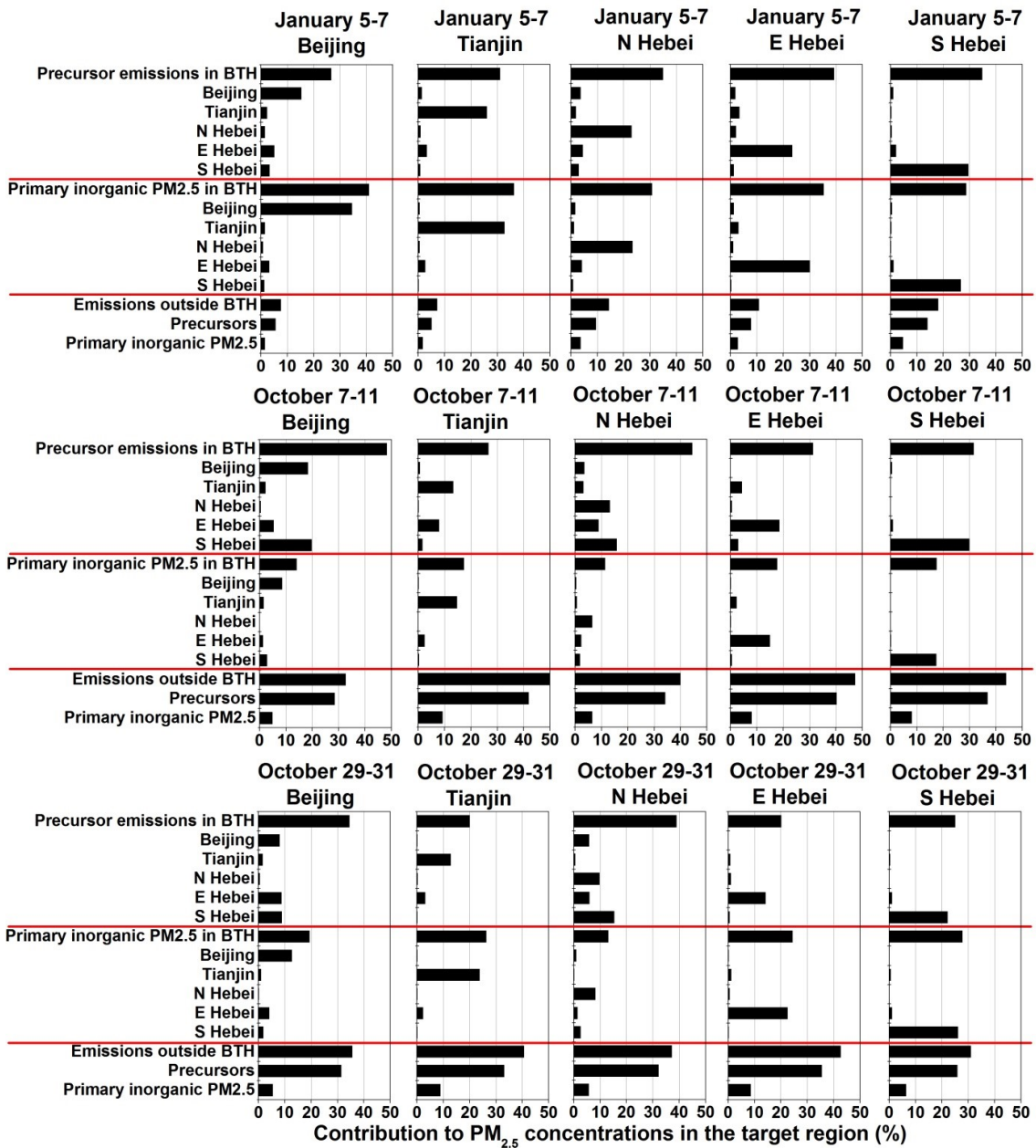
2

3 Figure 6. Contributions of precursor (NO<sub>x</sub>, SO<sub>2</sub>, NH<sub>3</sub>, NMVOC, IVOC, and POA) and  
 4 primary inorganic PM<sub>2.5</sub> emissions from individual regions to PM<sub>2.5</sub> concentrations. The  
 5 contributions are quantified by comparing the base case with sensitivity scenarios in which  
 6 emissions from a specific source are reduced by 80%. This figure illustrates contributions to  
 7 4-month mean PM<sub>2.5</sub> concentrations and monthly mean PM<sub>2.5</sub> concentrations in January and  
 8 July. The results for March and October are given in Fig. S6.



1 Figure 7. Sensitivity of monthly mean  $\text{NO}_3^-$ ,  $\text{SO}_4^{2-}$ , and OA concentrations to stepped control  
 2 of individual air pollutants in January and July. The meanings of X-axis, Y-axis, coloured  
 3 bars, black dotted lines, and red stars are the same as Fig. 4 but for  $\text{NO}_3^-/\text{SO}_4^{2-}/\text{OA}$ . The  
 4 results for March and October are given in Fig. S7.

5

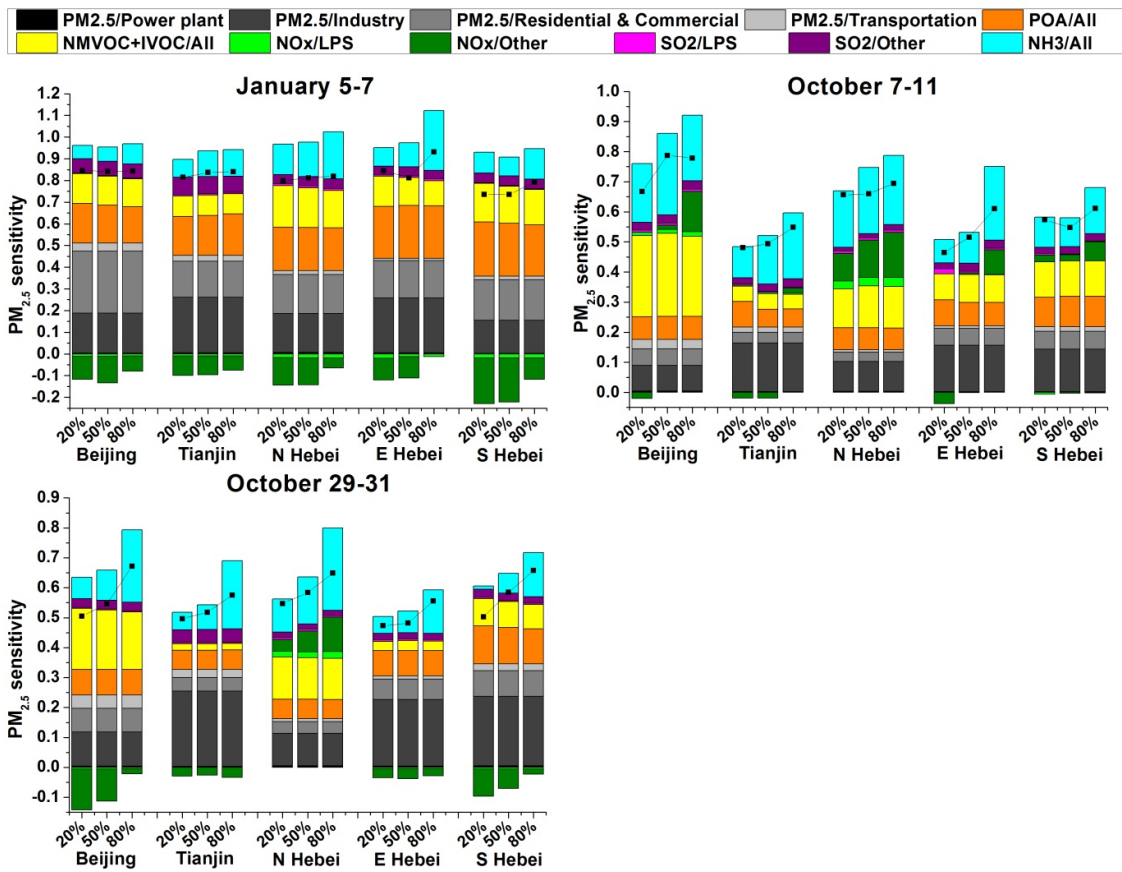


1

2

3 Figure 8. Contribution of precursor (NO<sub>x</sub>, SO<sub>2</sub>, NH<sub>3</sub>, NMVOC, IVOC, and POA) and primary  
 4 inorganic PM<sub>2.5</sub> emissions from individual regions to PM<sub>2.5</sub> concentrations during three  
 5 typical heavy-pollution episodes.

6



1  
 2 Figure 9. Sensitivity of  $PM_{2.5}$  concentrations to stepped control of individual air pollutants  
 3 from individual sectors during three heavy-pollution episodes. The meanings of X-axis, Y-  
 4 axis, coloured bars, and black dotted lines are the same as Fig. 4.

5